Predicting temperature-dependent transmission suitability of bluetongue virus in livestock

Fadoua El Moustaid[1,4], Zorian Thronton[2,3], Hani Slamani[2,3], Sadie J. Ryan[5, 6, 7], and Leah R. Johnson[1,2,3,4, *]

[1]Department of Biological Sciences, Virginia Tech, Blacksburg, VA 24061, USA

[2]Department of Statistics, Virginia Tech, Blacksburg, VA 24061, USA

[3]Computational Modeling and Data Analytics, Virginia Tech, Blacksburg, VA 24061, USA

[4]Global Change Center, Virginia Tech, Blacksburg, VA 24061, USA

[5]Quantitative Disease Ecology and Conservation (QDEC) Lab, Department of Geography, University of Florida, Gainesville, FL 32601

[6]Emerging Pathogens Institute, University of Florida, Gainesville, FL 32610

[7]School of Life Sciences, University of KwaZulu, Natal, South Africa

[*]Corresponding author: lrjohn@vt.edu

August 15, 2022

Abstract

The transmission of vector-borne diseases is governed by complex factors including pathogen characteristics, vector-host interactions, and environmental conditions. Temperature is a major driver for many vector-borne diseases including Bluetongue viral (BTV) disease, a midge-borne febrile disease of ruminants, notably livestock, whose etiology ranges from mild or asymptomatic to rapidly fatal, thus threatening animal agriculture and the economy of affected countries. Using modeling tools, we seek to predict where the transmission can occur based on suitable temperatures for BTV. We fit thermal performance curves to temperature-sensitive midge life-history traits, using a Bayesian approach. We incorporate these curves into $S(T)$, a transmission suitability metric derived from the disease's basic reproductive number, R_0. This suitability metric encompasses all components that are known to be temperature-dependent. We use trait responses for two species of key midge vectors, *Culicoides sonorensis* and *Culicoides variipennis* present in North America. Our results show that outbreaks of BTV are more likely between 15°C and 34°C with predicted peak transmission risk at 26°C. The greatest uncertainty in $S(T)$ is associated with: the uncertainty in mortality and fecundity of midges near optimal temperature for transmission; midges' probability of becoming infectious post-infection at the lower edge of the thermal range; and the biting rate together with vector competence at the higher edge of the thermal range. We compare three model formulations and show that incorporating thermal curves into all three leads to similar BTV risk predictions. To demonstrate the utility of this modeling approach, we created global suitability maps indicating the areas at high and long-term risk of BTV transmission, to assess risk and to anticipate potential locations of the establishment.

Author Summary

In this paper, we use data on traits of the biting midge that are sensitive to temperature to study bluetongue disease transmission. Bluetongue disease is a vector-borne disease that

threatens different types of ruminants, including sheep and cattle. This disease affects the livestock economy in the US and around the world. Here, we focus on two species of biting midges that transmit the bluetongue virus. First, we collect temperature-dependent trait data from previously published studies. Then, we used this data to derive the parameters incorporated into the mathematical and statistical models. To assess the transmission risk, we use a metric derived from the model to identify the temperature range suitable for bluetongue disease transmission. Our findings allow us to predict the areas around the world that could be at risk of bluetongue transmission should the midge species be present. These areas require more surveillance in case a bluetongue disease outbreak begins. Potentially, our results can inform future control and prevention strategies for bluetongue disease.

Keywords— Bluetongue virus, vector-borne diseases, transmission, Bayesian analysis, temperature, disease modeling

1 Introduction

With ongoing climate change, it is critical that we understand how temperature influences the dynamics of emerging diseases. Vector-borne diseases (VBDs) are highly sensitive to climate factors, particularly temperature, as demonstrated previously for VBDs of both humans and plants [1, 2, 3, 4, 5]. Bluetongue virus (BTV), in the *Reoviridae* family (genus *Orbivirus*), causes the disease Bluetongue in livestock across the world and is thus a VBD of considerable economic concern. The biting midges of the *Culicoides* family are responsible for transmitting BTV and many other arboviruses. More than 1,400 species of *Culicoides* have been classified, globally, but fewer than 30 have been identified as competent vectors for BTV transmission [6]. These midges are highly sensitive to changes in temperature [7, 8], and thus so is BTV transmission [9, 10].

BTV can infect most species of domestic and wild ruminants, including sheep, goats, and cattle [11]. Sheep are the most susceptible to the disease and exhibit the highest morbidity

and mortality, post-infection [12, 13]. In the majority of infections by strains of BTV's 27 serotypes, animals rarely show any clinical signs [14]. The infection severity and the presence of clinical signs both depend on the serotype, and the severity of infection can range from rapid fatality to quick recovery. Common outward clinical signs include a blue tongue, fever, and excessive salivation [13]. Since clinical signs are rare, BTV infection often goes without detection. Unfortunately, undetected cases can still result in mortality, and while BTV vaccines exist, vaccine development is in its infancy [15]. An effective polyvalent vaccine to immunize against more than one strain of BTV has yet to be developed [16], and existing attenuated viral vaccines pose significant health risks to livestock, such as reduced milk production in lactating sheep, abortion, early embryonic death, and teratogenesis in pregnant females [17].

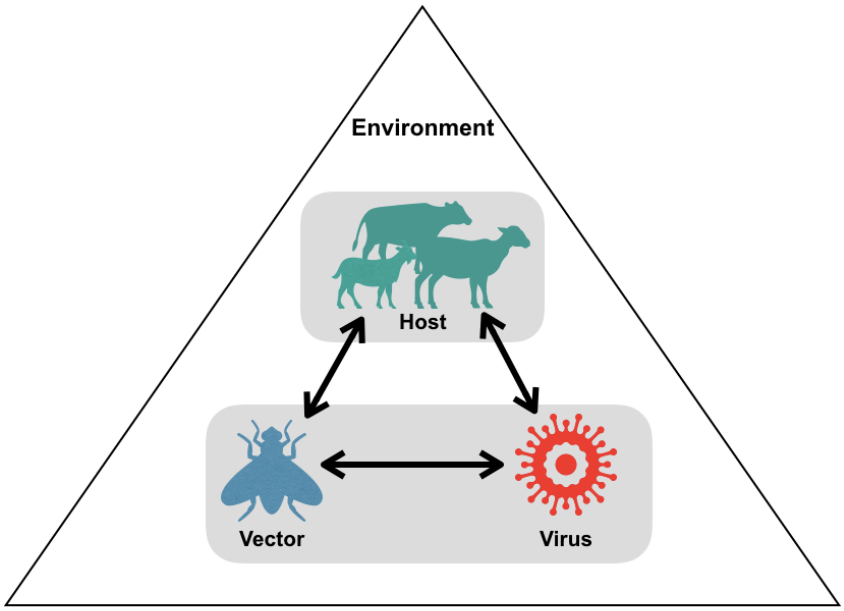

Figure 1: Bluetongue virus interaction diagram: the mechanisms underlying the transmission of bluetongue virus include, host-vector interactions, host-pathogen interactions, vector-pathogen interactions as well as the environmental effect on all interactions.

In the absence of an effective polyvalent BTV vaccine, and with the potential risks and costs of the available vaccines, the impact of BTV on global agriculture is significant. For example, the cost of BTV in the U.S. beef industry was estimated at $95 billion in 2014 [16]. Although BTV was first detected among merino wool sheep in South Africa in 1905, since

then the disease has been found on every continent but Antarctica [18]. In recent years, the disease has spread to areas previously believed to not be at risk, including North and Central Europe, parts of Asia, and Western North America [12, 19]. Mandatory testing of animals and losses in foreign markets form a huge economic burden. This adds to the economic impact of BTV on the livestock industry. There is substantial improvement needed in our ability to assess risks and to anticipate potential shifts in risk over time and space.

Though the cause of the recent appearance of BTV in some of the new regions (especially Northern Europe) is still unknown, it is believed that climate change is a major driver. More specifically, the increase in temperature of certain locations makes them suitable for midges to survive, and therefore transmit diseases [13]. For example, some cases of BTV-8 in Europe, specifically in France, have exceeded expectations of receding and survived cold winters [20].

Mathematical modeling can facilitate our understanding of the complexities of the transmission process of vector-borne diseases [10, 21, 22]. The classical Ross-MacDonald model of VBDs and similar models allow us to calculate the basic reproductive ratio R_0 of the disease [23, 24]. This summary quantity is widely used to estimate how infectious a disease is and whether an outbreak can occur. When $R_0 > 1$, the disease is likely to spread, leading to an outbreak; when $R_0 < 1$ the disease is likely to die out. As shown in Figure 1, BTV transmission involves host-vector interactions, host-virus interactions, vector-virus interactions, and the effect of the environment. Mathematical models allow us to describe these interactions, parameterize them with data, and quantify the knock-on effects for transmission risk.

Here we are interested in answering the following questions: (1) How does the risk of transmission of BTV vary with temperature? (2) Do different model assumptions lead to different predicted suitability ranges? and (3) Which traits contribute the most to variation in estimates of transmission risk? To answer these questions, we take an approach used previously for VBDs such as malaria [1, 2]. We begin by using Bayesian inference to fit thermal responses to laboratory-derived data for temperature-sensitive midge life-history traits. We then derive R_0 for BTV as a function of these thermal responses and incorporate the fitted

thermal responses to obtain estimates of these across temperatures. To focus on just the temperature-dependent components, we define a suitability metric, $S(T)$, that isolates the temperature-sensitive components of R_0. We compare forms of $S(T)$ where the midge density, V, is constant vs temperature-sensitive to ascertain if this generates major differences in suitability predictions. Next, we conduct uncertainty analyses to assess identify which parameters drive uncertainty in $S(T)$. This can indicate that either further data collection is needed to refine estimates, or that certain parameters have greater impacts on BTV disease transmission at different temperatures. Finally, we visualize predictions of the fitted suitability framework to explore which geographical areas might be suitable for transmission in the current native range of the midges, or if they become established elsewhere. Furthermore, understanding which temperature range results in $S(T) > 0$, for given levels of other fixed parameters in our model, may inform prevention and control strategies that target particular parameters (e.g., adult mortality rates via pesticide application).

2 Methods

2.1 Derivation of R_0 and $S(T)$

To predict the outbreak potential of BTV, several forms of the basic reproductive number R_0 have been developed [10, 21, 22]. The classical reproductive ratio for a generic VBD [1, 25] is given by

$$R_0 = \left(\frac{V\ bc\ a^2}{d\ H\ \mu} e^{-\mu/\nu} \right)^{1/2} \quad \text{from} \quad [25] \tag{1}$$

where V is midge population density; bc is vector competence (the product of the probability that a midge can transmit the infection to an uninfected host, b, and the probability that a midge gets infected when biting an infected host, c); a is the per-midge biting rate; μ is the adult midge mortality rate; ν is the pathogen development rate ($\nu = 1/EIP$ with EIP the extrinsic incubation period); H is host density, and d is infected host recovery rate.

The model used to derive this version of R_0 is a system of delay differential equations that assumes no exposed class and that susceptible midges move to the infected class shortly after contact with an infected host. A similar scenario can be described using a system of ordinary differential equations while expressing the delay between the contact with infected host and midges becoming infectious in terms of an exposed class. In this case, the reproductive number for the midge-borne viral disease (BTV) can be expressed as,

$$R_0 = \left(\frac{V\ bc\ a^2}{d\ H\ \mu} \frac{\nu}{\nu + \mu} \right)^{1/2} \quad \text{from} \quad [10] \tag{2}$$

This version of R_0 is a reduced version from a model that uses multiple types of host and multiple types of midge species as in [10, 21].

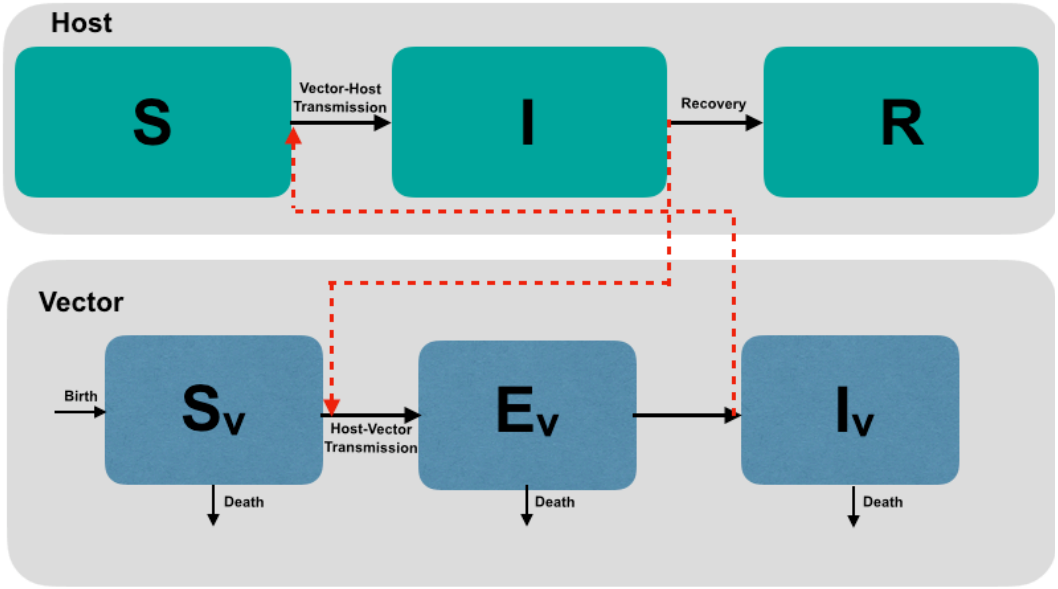

Figure 2: A schematic illustration of BTV transmission. The host population is composed of three classes: susceptible (S), infected (I), and recovered (R). The midge population is composed of a susceptible class (S_v), three exposed classes (E_v), and an infected class (I_v). Black arrows show movement between classes and red arrows indicate contact potentially leading to transmission.

Figure 2 shows a schematic representation of our BTV transmission model (Equations (1)-(8) in Appendix A) which considers a single host population split into susceptible individuals that are vulnerable to BTV disease (S), infected individuals that have acquired infection (I), and individuals who have recovered from the disease (R). Also, we consider a vector

population containing susceptible midges (S_v), three levels of exposed individuals (E_v), and an infected class of midges (I_v). The exposed classes in the model represent the extrinsic incubation period that midges undergo before becoming able to transmit infection. To calculate the third version of the basic reproductive number R_0, we use a next-generation matrix method described in [26, 27], which leads to the following R_0 equation:

$$R_0 = \left(\frac{V\ bc\ a^2}{d\ H\ \mu} \left(\frac{3\ \nu}{3\ \nu + \mu} \right)^3 \right)^{1/2}. \tag{3}$$

The term $\left(\frac{3\ \nu}{3\ \nu + \mu} \right)^3$ in R_0 represents the number of midges that survive the extrinsic incubation period, leading to a slight difference between the three R_0 forms.

We can represent all three formulas of R_0 with a simple equation given by

$$R_0 = \left(\frac{Vgf}{d\ H\ \mu} \right)^{1/2} \tag{4}$$

$$= \left(\frac{(midge\ density)\ \overbrace{(transmission\ potential)}^{g}\ \overbrace{(prob\ of\ becoming\ infectious)}^{f}}{(host\ recovery\ rate)\ (host\ density)\ (vector\ mortality)} \right)^{1/2} \tag{5}$$

where the expression for V and g are the same for all three versions and are given by

$$V = \frac{F\ p_E\ p_L\ p_P}{\mu^2\ (\rho_E + \rho_L + \rho_P)} \tag{6}$$

$$g = a^2\ bc \tag{7}$$

where F is eggs per female per day, p_E, p_L, and p_P are survival probabilities for eggs, larvae, and pupae; ρ_E, ρ_L, and ρ_P are development times for eggs, larvae, and pupae, respectively; μ is adult midge mortality; a is midge biting rate and bc is midge competence.

Although R_0 is a useful metric, particularly since the thresholding behavior can predict whether or not an epidemic can take hold, multiple factors, including the size of the susceptible population, whether or not parasites/hosts/vectors are physically present in an

area, socio-economic factors (e.g., screens, household and working conditions), or control measures, can all impact R_0 at a particular location. We want to focus our analysis strictly on the temperature components of the transmission, to be able to determine the temperatures that prohibit or promote transmission, and explore sensitivity to the thermal traits independently of other factors. Thus, we define a transmission suitability metric, $S(T)$, as the (standardized) thermal components of R_0 (Equation 4), which is given by

$$\begin{aligned} S(T) &= C\left(\frac{Vgf}{\mu}\right)^{1/2} \\ &= C\left(\frac{F\ p_E\ p_L\ p_P\ a^2\ bc\ f}{\mu^3\ (\rho_E+\rho_L+\rho_P)}\right)^{1/2} \end{aligned} \tag{8}$$

where C is a constant that is chosen after the Bayesian fitting of traits (see below) that scales the median suitability to lie between 0 and 1. That is, we choose C to be the highest value of the posterior median suitability. When the median suitability is zero this indicates that temperatures do not permit transmission and when the median suitability is 1, this indicates a maximal transmission, everything else being equal.

The difference between the three $R_0/S(T)$ formulas lies in the latent period survival probabilities, f, representing the probability of midges surviving to become infectious post-infection. Table 1 summarizes the latent period survival probabilities for each of the three models considered.

In Figure 3, we plot all three latent period survival probabilities with one parameter fixed as the other varies (e.g., with virus development rate, ν, fixed and midge mortality rate, μ, varying). We use all three forms in our analysis while comparing the constant vector density case V to temperature-sensitive density $V(T)$.

2.2 Bayesian fitting of temperature-sensitive traits

As ectotherms, midges are sensitive to temperature. The thermal performance for these temperature-dependent traits is generally hump-shaped, starting at zero at a given minimum

Formula	Traits Used
$f_1 = e^{-\mu\,\nu}$ [Dietz 1993]	μ : adult mortality rate
$f_2 = \dfrac{\nu}{\nu+\mu}$ [Gubbins et. al. 2008]	ν : pathogen development rate
$f_3 = \left(\dfrac{3\nu}{3\nu+\mu}\right)^3$	

Table 1: Formulas for the probability of an infected midge (vector) surviving to become infectious, arising in R_0 formulas from different models, and the parameters involved.

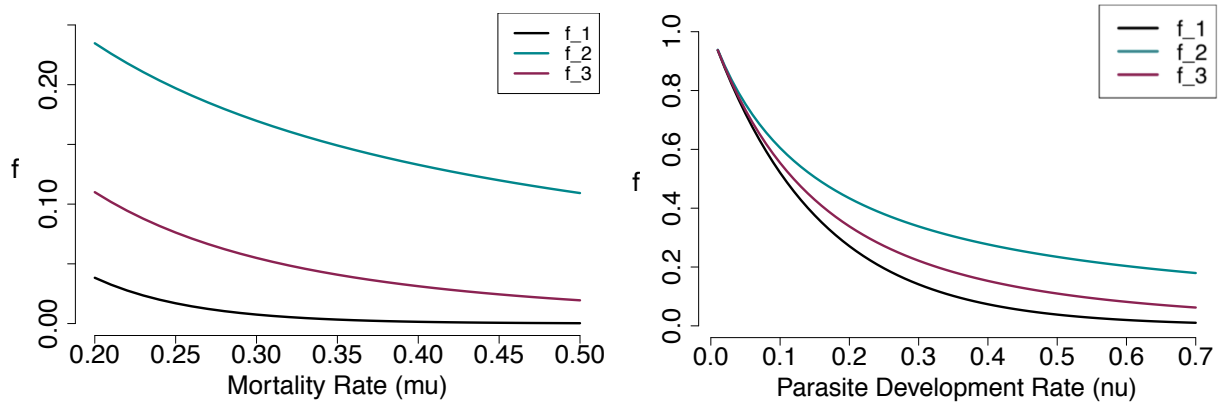

Figure 3: (Left) Latent period survival probability f versus midge mortality rate μ with a fixed $\nu = \text{mean}(\nu(T)) = 0.061$. (Right) Latent period survival probability f versus pathogen development rate ν with a fixed $\mu = \text{mean}(\mu(T)) = 0.15$

temperature, then increasing to a peak value as temperature increases, then sharply dropping to a lower value at a maximum temperature [28, 29]. However, depending on how a trait is measured, the pattern may instead be concave up. For example, mortality rates exhibit this pattern, such that the mortality is lowest at intermediate temperatures.

Here, we collected trait data corresponding to two midge species from the family *Culicoides*, namely, *Culicoides sonorensis* and *Culicoides variipennis*, both found the US [30]. The data collection method consisted of synthesizing data from published literature, via assembling data from tables, and digitizing data points from graphs; details on data used for fitting for each trait are provided in Appendix A. We focused on data from controlled

laboratory experiments on midge trait variation at constant temperatures, ideally with three or more data points. For digitization, we used the free software PlotDigitizer [31].

We used the temperature-dependent trait fits in all three $R_0/S(T)$ formulations for comparison. Following a method first introduced in [1], we fit unimodal curves to temperature-sensitive traits. For the unimodal curves, we chose between a Brière (Equation (9)) for left-skewed data or a quadratic formula (Equation (10)) for symmetric traits.

$$\text{Brière: } kT(T - T_{Min})\sqrt{T_{Max} - T} \tag{9}$$

$$\text{Quadratic: } inter - n.slope\ T + qd\ T^2 \tag{10}$$

where the constants k, T_{Min}, T_{Max}, $inter$, $n.slope$, and qd estimated from trait data.For more information on the values, see Appendix A.

Similarly to [2], we used a Bayesian approach for our fitting method. For each continuous positive trait, we choose a truncated normal distribution as our likelihood. When fitting probabilities/proportions, we instead either used a binomial likelihood (when raw count data was available) or used a normal likelihood truncated at zero and one if only summarized data were available. We chose priors for thermal performance curve (TPC) parameters to assure parameters have biologically reasonable sign and range.

We used Markov Chain Monte Carlo (MCMC) sampling in JAGS/rjags to fit our models [32]. For each trait, we ran five MCMC chains with 5000 step burn-in followed by 25000 samples. Of these we kept every fifth sample, to obtain 5000 thinned samples for subsequent analyses. We used these 5000 samples of each parameter to calculate the associated trait thermal curves, resulting in 5000 thermal fits of the trait data. After generating the 5000 posterior mean curves for each trait, we used the 5000 posterior curves to generate posterior curves for $R_0/S(T)$. For all posteriors (i.e., of traits and $S(T)$), we summarized posterior distributions using the temperature-dependent medians and the corresponding 95% highest posterior density (HPD) interval which is the smallest credible interval in which 95% of the

distribution lies [33]. All analyses were implemented in R [34]. More details on likelihoods and priors used can be found in Appendix A.

2.3 Uncertainty in $S(T)$

The $S(T)$ formula (Equation 8) depends on multiple temperature-sensitive traits, and so does its posterior density. Hence, there are many sources of uncertainty in the mean posterior density that can be identified through uncertainty analysis. We sought to isolate the contributions of each component of the model to the overall uncertainty through a variation on a traditional sensitivity analysis.

We calculated the uncertainty associated with f, g, and V by varying one while keeping the rest fixed at their posterior means. We calculated the width of the 95% credible interval around the mean posterior curve, i.e. the difference between the upper and lower quantiles when only one of the components is allowed to vary. We then divide this by the width of the interval when all are allowed to vary. We repeat this process for each component, f, g, and V then plot all the curves together against temperature. This allows us to identify which model component is responsible for the largest proportions of uncertainty in $S(T)$ by identifying the curve with the highest value at a given temperature.

2.4 Mapping suitability

The concern about climate-mediated increases and shifts in BTV risk is best visualized using mapping approaches, to understand where suitability is permitted and for how long, and how much livestock are thus at risk. Existing mapping approaches to this question largely focus on the European landscape, due to recent upticks in BTV outbreaks. However, existing models purport to capture a general *Culicoides spp.* model but must rely on data from the U.K. vector *Culicoides obsoletus* mixed with other species that may not be the dominant vector, or even currently present. In this study, we focus on the two US vectors for which there are data and project a global risk. We do this under the assumption that given

the capacity for *Culicoides* to spread and establish – as demonstrated by the Afro-tropical *C. imicola* invasion across Southern Europe in recent decades – there may well be similar invasions and establishment by the two well-studied U.S. vectors, and thus specific models will provide useful planning tools.

To visualize and apply our understanding of the thermal suitability of BTV, we mapped both suitability and risk, at global scales. First, we define suitable regions as those where the posterior median of the suitability metric $S(T)$ >0. This is equivalent to finding the values where the posterior probability that $S(T) > 0$ is 0.5. We note that here we use a scaled form of $S(T)$ as we described above. We present the geography of suitability across the globe by mapping the number of months of suitable temperatures for transmission based on the monthly average temperatures from the WorldClim dataset [35]. We use these average monthly temperatures as a means to describe seasonality, at a global scale, with climate products that are comparable between baseline (current temperatures) and future scenarios, to lay the groundwork for future investigations. The WorldClim data provide a trade-off between a spatial and temporal resolution that facilitates conducting calculations of risk across the globe.

Second, we map livestock at risk of transmission, using the latest FAO Gridded Livestock of the World (GLW3) data for 2010, which details global distributions of sheep, goats, cows, and others, at a 5-minute scale [36]. To create a visually accessible risk map, suitability was scaled 0-1, and this was multiplied by $log_{10}(1 +$ livestock). Thus we create a scaled risk map, balancing the season length and livestock density, to emphasize areas of coincidence, rather than simple suitability. In this case, we used the GLW3 sheep distribution [37], as the primary host at risk. This gridded product has values ranging from 0 - >340,000 sheep per pixel. All map calculations and manipulations were run in R using packages raster [38, 39], maptools [40] and Rgdal [41], following methods described in [42, 43].

3 Results

3.1 Temperature-dependence model components

Here we summarize the model components that depend on temperature and explain their role in the model.

Midge thermal traits

In Figure 4 we show data and fitted curves for development times and survival probability for eggs, larvae, and pupae. Development times Figure 4 (left) are fitted assuming a quadratic function, under the assumption that juvenile midges at a given stage will need more time to develop at very low (<20°C) and very high (>35°C) temperatures. For eggs, the development time ranges from 60 to 70 days; for larvae, from 15 to 35 days; and for pupae between 40 and 80 days. We fit the survival probabilities using a Brière curve (Figure 4 right). The survival probability is relatively high for eggs ($0.2 < p_E < 0.8$), very low for larvae ($p_L < 0.2$), but almost always 100% for the pupae stage ($p_P \sim 1$).

In Figure 5 A, we show data on fecundity F (the number of eggs laid per female per day) together with the fitted Brière curve. The fecundity reaches a maximum at $\sim$ 30°C and we do not have data for temperatures beyond that. The mortality rate, μ, is fit using a quadratic curve where we assume that the mortality is highest for temperature less than 10°C and higher than 30°C (Figure 5 B).

Figure 6 we show the biting rate a and the transmission probability b both fit with a Brière curve. The biting rate minimal values lie around 10°C and increase to reach a maximum at 30°C. While the transmission probability b is minimal around 15°C and reaches a maximum at 30°C. We do not have data for the infection probability c so we assume that it is equal to 0.5. Lastly, Figure 7 shows the virus development rate fit using a Brière curve, with minimal values around 15°C and maximal values around 32°C. Overall, these thermal traits all lack data values at extreme temperatures.

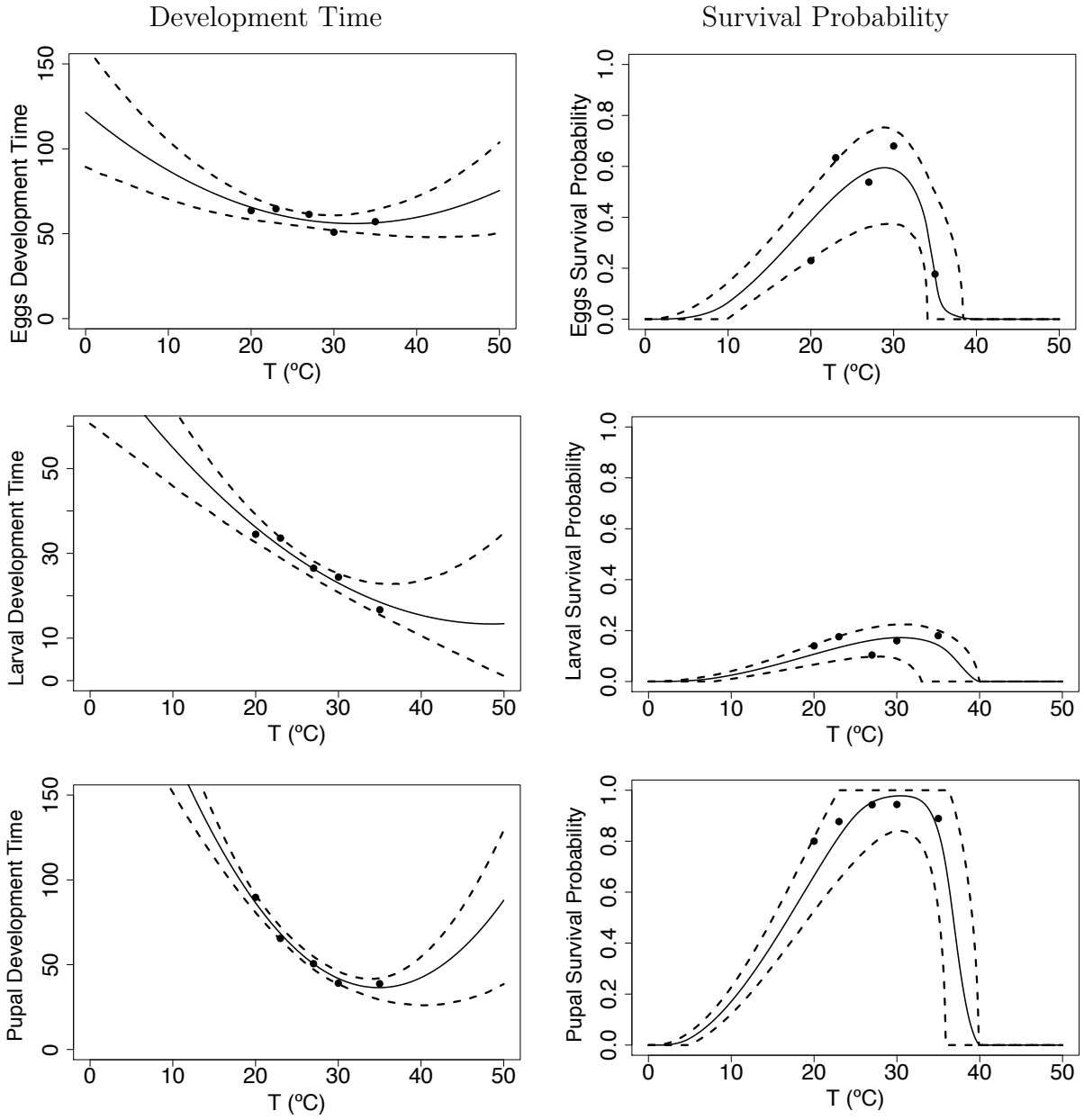

Figure 4: Figures in the LEFT panels show development time in days for midge juvenile stages, eggs ρ_E, larvae ρ_L, and pupae ρ_P. Figures in in the RIGHT panels show survival probabilities for midge juvenile stages, eggs p_E, larvae p_L, and pupae p_P. The solid line is the mean of the posterior distributions of the thermal response curves while the dashed lines represent the HPD intervals

Midge density V

Recall the midge density formula given by

$$V(T) = \frac{F(T)\, p_E(T)\, p_L(T)\, p_P(T)}{\mu(T)^2\, (\rho_E(T) + \rho_L(T) + \rho_P(T))} \tag{11}$$

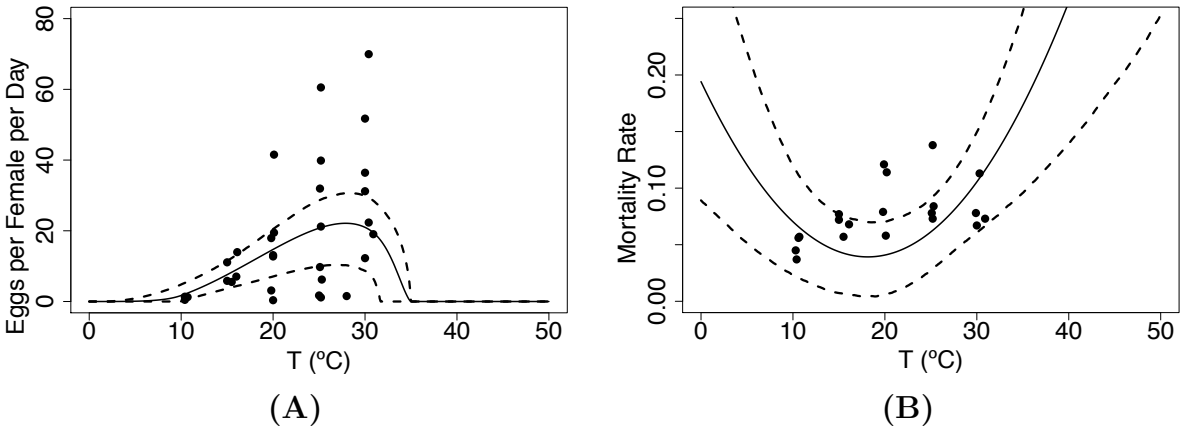

Figure 5: (A) Fecundity, F (Eggs per female per day) and (B) adult mortality rate μ traits as they vary with temperature. The solid line is the mean of the posterior distributions of the thermal response curves while the dashed lines represent the HPD intervals

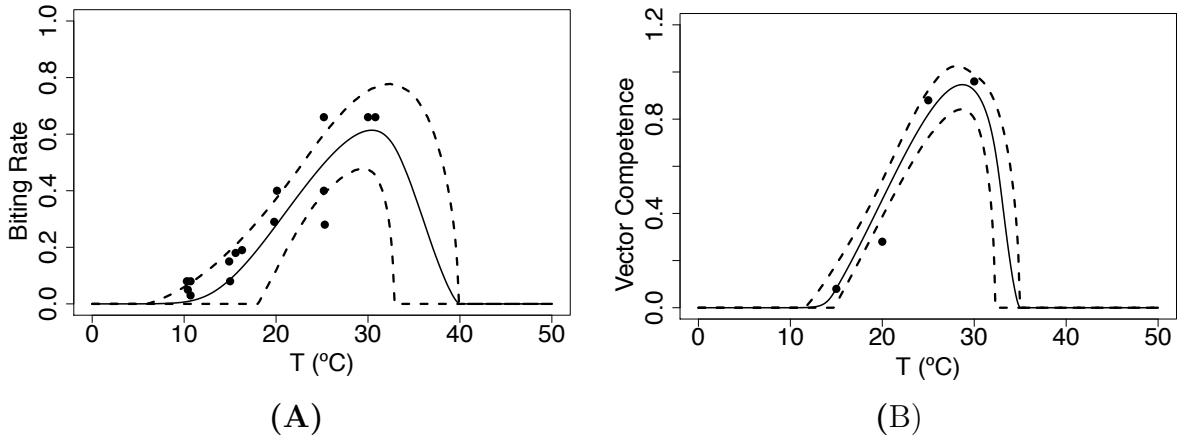

Figure 6: (A) Biting rate a and (B) probability that midges transmit infection when biting an uninfected host b. The solid line is the mean of the posterior distributions of the thermal response curves while the dashed lines represent the HPD intervals

To estimate midge density V, we use the posterior samples of the survival probabilities $p_E,\ p_L,\ p_P$, for egg, larvae, and pupae; the development times $\rho_E,\ \rho_L,\ \rho_P$ corresponding to the egg, larvae, and pupae life stages; the fecundity measure represented by the number of eggs per female per day F; and the adult mortality rate μ. In Figure 8 we show that the posterior estimate of temperature-dependent midge density V is highest between 20 °C and 28 °C; it increases at temperatures higher than 10 °C and decreases when the temperature exceeds 28 °C.

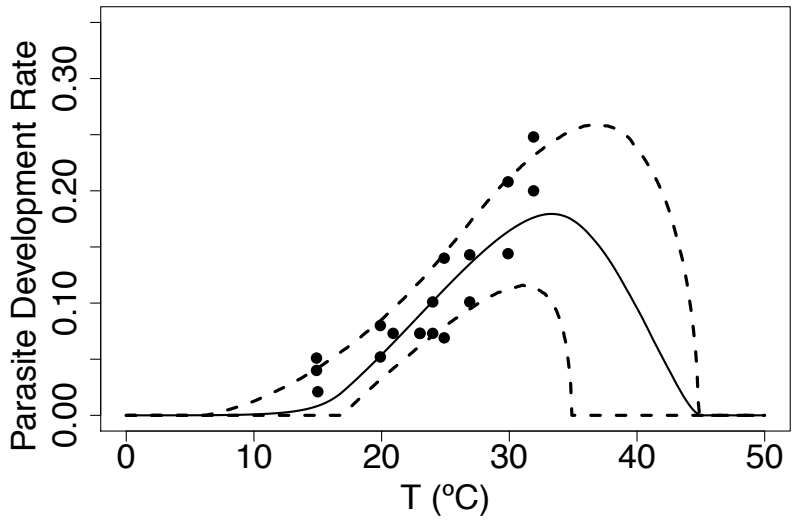

Figure 7: Virus development rate (ν) is the inverse of extrinsic incubation period ($\nu = 1/EIP$). The solid line is the mean of the posterior distributions of the thermal response curves while the dashed lines represent the HPD intervals

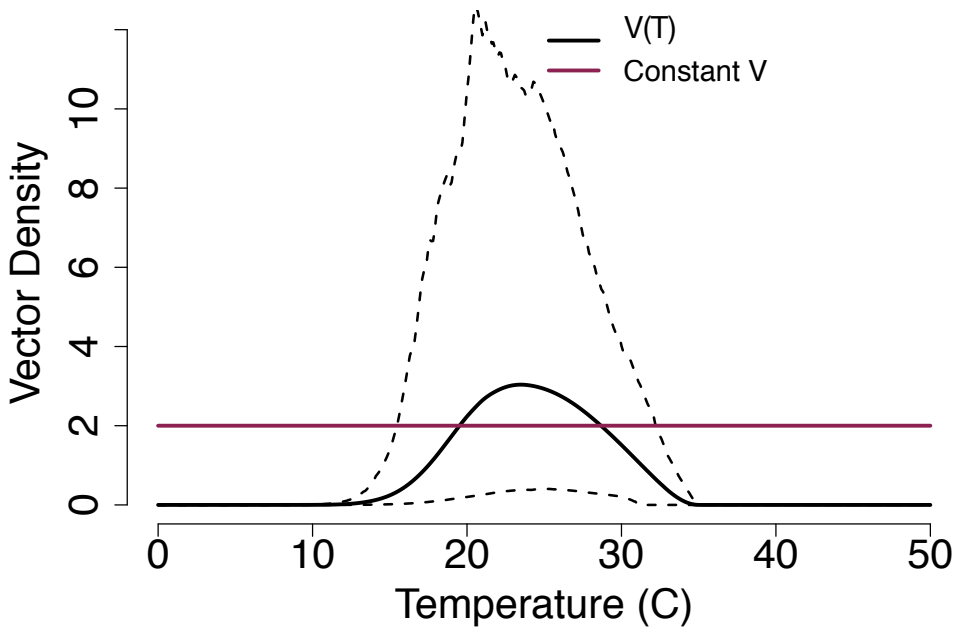

Figure 8: Modeled midge density as it varies with temperature. To obtain the temperature-dependent midge density, V(T), we evaluate Equation 11 at all temperature-dependent traits using the fitted curves. The solid black line shows the estimated density and the dashed lines show the corresponding HPD interval. A constant value $V = 2$ is shown for comparison for subsequent modeling where the density is constant.

Transmission potential

The component g, that we call the transmission potential, is estimated by calculating the product of midge biting rate a and vector competence bc:

$$g(T) = b(T)c\, a^2(T); \tag{12}$$

Temperature-dependent data the transmission probability c was unavailable. Thus we assumed that there will be a 50% chance for midges to become infected after biting an infected host ($c = 0.5$) regardless of temperature. Figure 9 shows the posterior distribution of the predicted transmission potential thermal curve.

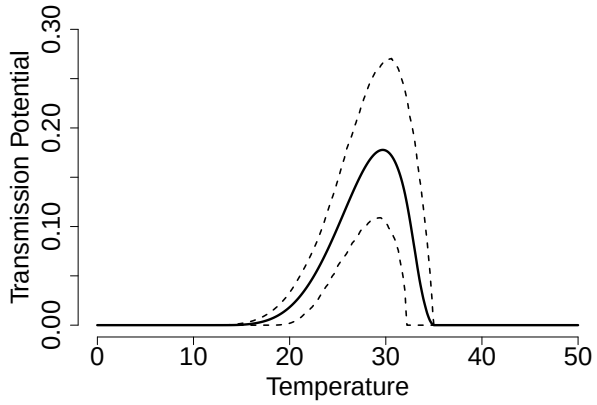

Figure 9: The transmission potential g as the biting rate a and transmission probability b vary with temperature while the infection probability is constant $c = 0.5$. The solid line shows the estimated curve and dashed lines are the HPD interval.

Functional form

We explored three functional forms of the formula used to represent the probability of midges surviving to become infectious (Table 1). In all three cases, we calculate the thermal dependence of the functional form using the posterior distributions of mortality rate μ (Figure 5 (B)), and virus development rate ν (Figure 7). Figure 10 shows the variation of the functional form with temperature based on the two temperature-dependent traits μ and ν. Although there are differences between the magnitude of these curves, we can see that their peak occurs at the same temperature (25 °C), which is due to the traits' thermal dependencies. In addition, all of their HPD intervals overlap which means that there are no significant differences between them.

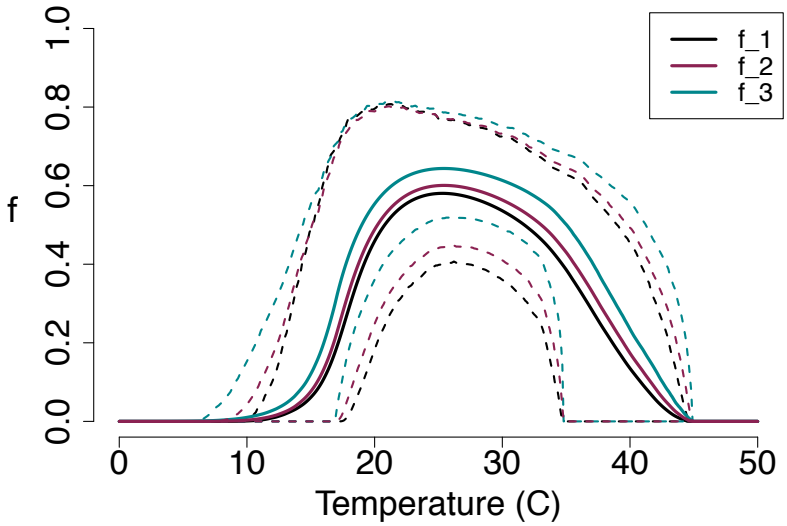

Figure 10: Latent period survival probability f used in R_0 versus temperature. The black line shows our model with the newly derived R_0, the purple line shows the model presented in [10], and the blue line shows the model presented in [25]. Each solid line represents a different model and the dashed lines show the corresponding HPD intervals. We note that there is an overlap between all HPD intervals meaning that there are no statistically significant differences between these models.

3.2 Thermal Suitability $S(T)$

We use thermal traits to evaluate $S(T)$ given by Equation 8 with constant midge density V (Figure 11 Top) and with temperature-dependent midge density $V(T)$ (Figure 11 Bottom). The three models are slightly different when constant midge density is used but are in agreement when temperature-dependent midge density is used. This is due to all the temperature-sensitive traits used to calculate $V(T)$; however, this also leads to a higher uncertainty shown in the range of HPD interval in Figure 11 (Bottom). The lower thermal bound of the three posterior means are different by a magnitude of 1°C. However, the peak temperature and upper thermal limits are in agreement for all three models. With these results, we predict that $S(T) > 0$ occurs at a temperature greater than 15°C and less than 34°C, meaning that BTV is likely to cause an outbreak within this temperature range. We note that this prediction is based on assuming $c = 0.5$ which may not be always true in reality.

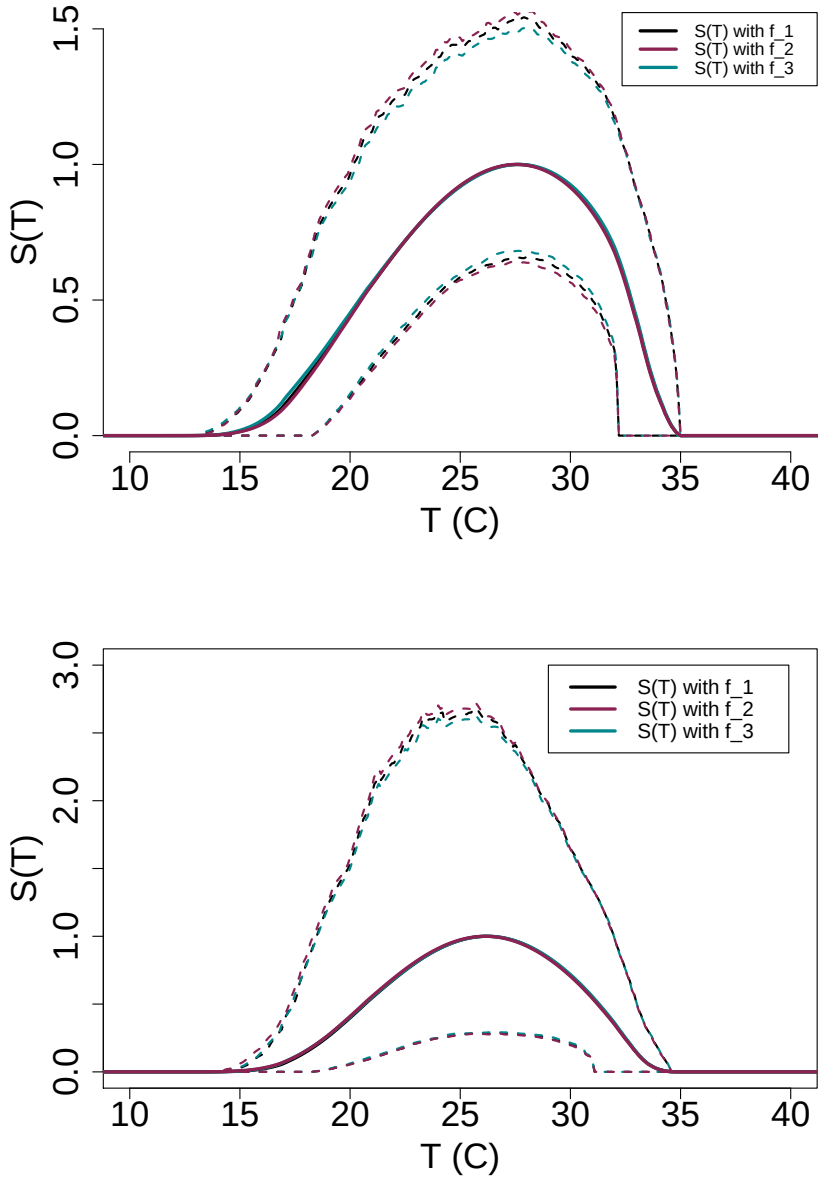

Figure 11: (Top) $S(T)$ with constant midge density V and (Bottom) $S(T)$ with temperature-dependent midge density $V(T)$. The plots shows the magnitude of $S(T)$ changing as temperature increases. Each solid line represent the mean of the posterior distributions of R_0 while the dashed lines are the HPD intervals.

3.3 Source of uncertainty in $S(T)$

In Figure 11 (Bottom), a high variation around $S(T)$ posterior density is shown in the large HPD interval. To determine the source of this uncertainty, we plot the calculated relative widths for each $S(T)$ component, see Figure 12. The results show that at a low-temperature

range ($14°C < T < 18°C$) uncertainty in $S(T)$ is mainly due to the uncertainty in the functional form$f$. At intermediate temperatures ($18°C < T < 33°C$), the uncertainty is caused by the midge density $V(T)$. At very high temperatures ($33°C < T < 35°C$), the transmission potential g is the component producing the most variability in $S(T)$.

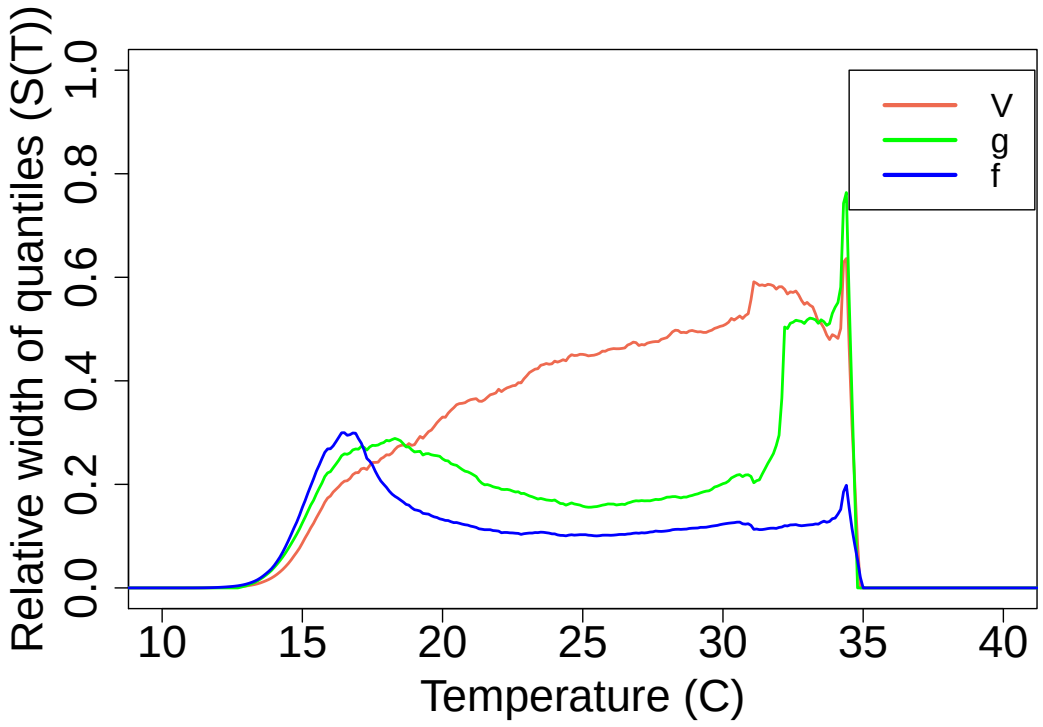

Figure 12: The source of uncertainty in $S(T)$ is measured by calculating the relative width of the 95% HPD quantiles with each component varying with temperature while the remaining components are kept constants, and divided by the width when all are allowed to vary.

3.4 BTV risk maps

Figure 13 illustrates the number of months each area is at risk of BTV transmission with the assumption that *Culicoides sonorensis* and *Culicoides variipennis* are the main vectors. The results show that, under baseline long-term average current temperature conditions, much of central Africa, South Asia, central and the northern part of South America, and northern Australia are suitable for year-round bluetongue transmission. These areas are also

the warmest parts of the world, and as we move away from them, the temperature is lower and the number of months of suitability is reduced.

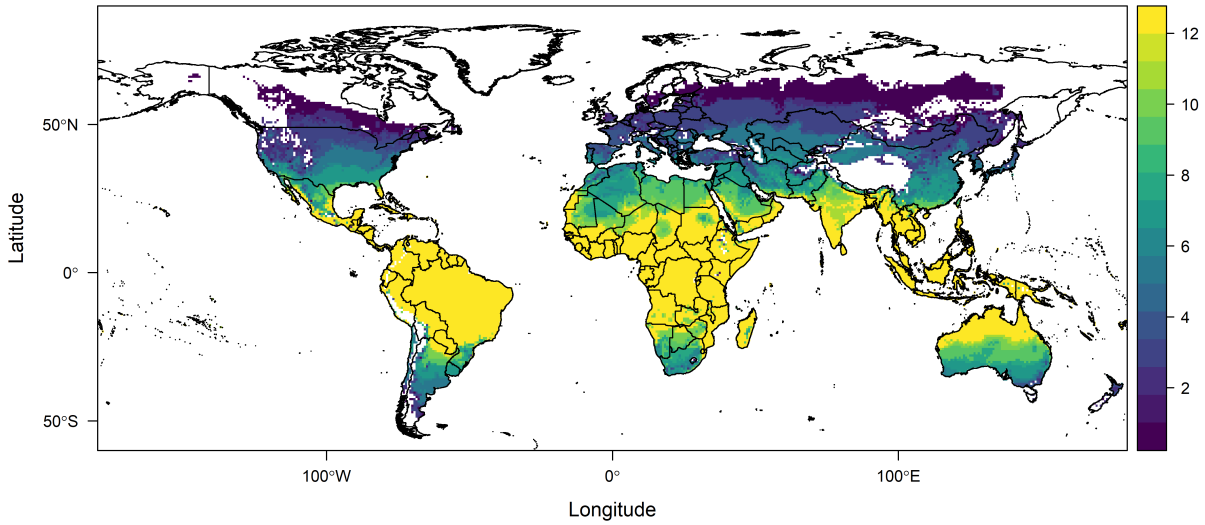

Figure 13: Map of the number of months (1-12) areas are at risk of bluetongue virus transmission according to our temperature-dependent R_0. This map based on the current mean monthly temperatures and is restricted to bluetongue disease caused by the two midge species *Culicoides sonorensis* and *Culicoides variipennis*.

Next, we used the global distribution of sheep to determine areas where sheep are at risk of acquiring BTV. The choice of sheep was mainly due to ready data availability, and also because sheep are the BTV host with the highest mortality and morbidity rates, and therefore of great interest and relevance. The map shows that areas, where sheep are at the highest risk (scale > 3), are located around the equator. The next highest risk regions ($1 <$ scale < 3) are areas with of high livestock industry, such as central and south America and Europe.

4 Discussion

In this study, we are interested in the potential for the temperature to shape where BTV may spread. We use a Ross-Macdonald type modeling approach to describe the dynamics of BTV transmission [23, 24]. This mechanistic approach allowed us to derive the basic reproduction

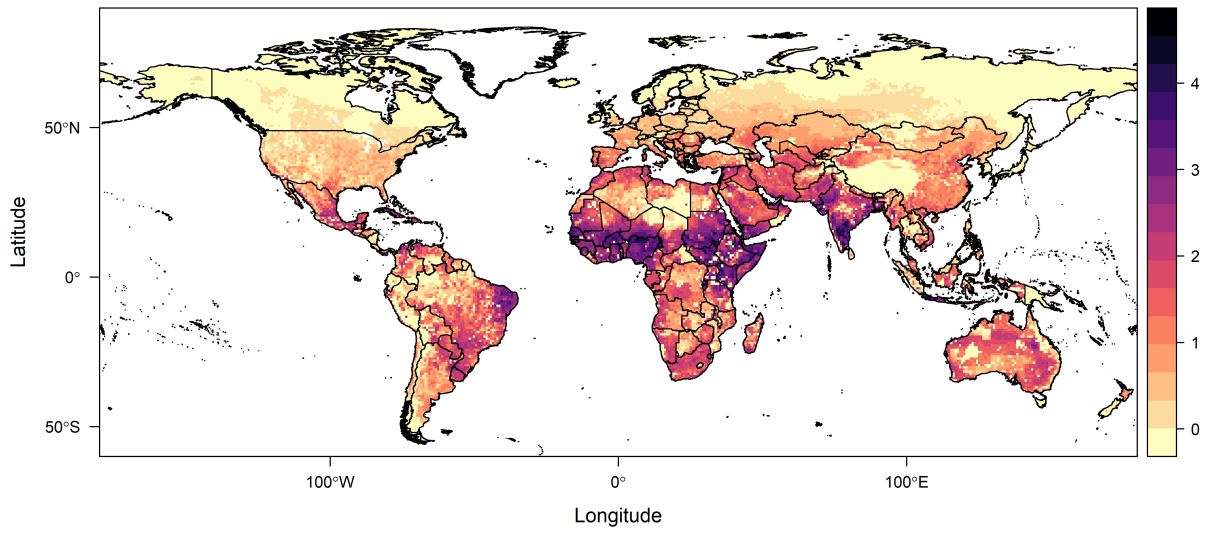

Figure 14: Scaled transmission risk suitability of bluetongue virus for sheep, as the primary host at risk, worldwide. the scale ranges from a low risk, 0, to a high risk, 5.

ratio's posterior distribution as a function of temperature. We were able to both determine the suitable temperature for possible BTV outbreaks when $S(T) > 0$ and the temperatures at which BTV outbreaks are likely to die out when $S(T) = 0$. We note that the absolute magnitude of the thermal response of $S(T)$ here is dependent on our model assumptions, for example setting the infection probability to be $c = 0.5$. We also adopt two previously used BTV models, [25] and [10], to compare the three forms of R_0.

Based on the available trait data we used in our model, we predict that temperatures from 15°C and 34°C, are "suitable" for BTV outbreaks by the examined midge species, with peak suitability occurring at about 26°C. This result was obtained regardless of which $S(T)$ formula used, i.e., all three different models of the latent period survival probability, f lead to the same predictions. Similarly, the predicted peak and upper thermal limit of $S(T)$ were the same for three forms, and only a small difference between lower thermal limits ($\sim$1 °C) was observed. This indicates that the uncertainty of temperature effects on traits outweigh the effects of differences in modeling assumptions in the form of the latent period survival probability for these models. Because our suitability metric captures all of the temperature-depend portions of R_0, this result should also hold for R_0 more broadly.

Uncertainty in temperature-dependent traits of the vector-virus system results in uncertainty in the suitability metric $S(T)$. Our uncertainty analysis allowed us to determine the traits responsible for causing uncertainty in $S(T)$ (and therefore in the temperature-depend components of R_0) across the temperature range. At lower temperatures ($14°C < T < 18°C$) more data are needed for the parasite development rate, ν, and mortality rate, μ, to reduce this uncertainty in the latent period survival probability, f. At moderate temperatures ($18°C < T < 34°C$) the uncertainty in $S(T)$ is caused by V, meaning that more data are needed in traits contributing to estimating the midge density. At very high temperatures ($34°C < T < 35°C$) we need more data on vector competence bc and biting rate a. Reducing the uncertainty in these components of $S(T)$ will allow refinement of predictions, control, and prevention suggestions.

We were interested in using our derived suitability metric to determine areas at risk of BTV based primarily on temperature suitability. A risk map can be a useful planning tool, both to understand the scale of current risk, and to anticipate suitable regions where the establishment of BTV could be successful were it to be introduced, with competent vectors. We created global risk maps showing the number of months per year each location worldwide is suitable for BTV disease transmission given the presence of two midge species, namely, *Culicoides sonorensis* and *Culicoides variipennis*. The results show that warmer areas are at risk year-round, while cooler areas are at risk for fewer months. Based on currently available data, few locations are predicted to have temperatures hot enough to exclude BTV for many months of the year. Further trait data to decrease the uncertainty near the thermal limits would enable more precise and accurate predictions. However, the particular predictions are also based on long-term, baseline current temperatures. With climate change, and the continuous rising of global temperatures, the area at risk of BTV may expand and shift to include places with previously lower risk, or some year-round locations may become too hot for year-round transmission [44, 45].

In building our maps, we chose to use monthly mean temperatures, as this captures the

mean response of the suitability determined mechanistically. Other approaches might be to use climate products with different temporal resolutions and express suitability in the number of days between thresholds, but these products tend to be available at much coarser spatial resolutions, making them less suitable for combining with livestock layers. Instinctively, one may want to use minimum or maximum temperatures to impose thresholds, but this faces a very biological conundrum of model mechanics - a minimum or maximum temperature may exist for a very small time period within a given month, and thus not represent a longer period experienced by the vector in question. The behavioral avoidance mechanisms vectors can use in short periods of extremes would be missed by this approach, leading to underestimates of the potential extent of suitability.

Previous studies have investigated temperatures suitable for other vector-borne diseases. For example, a study on three mosquito-borne diseases, Zika, dengue, and chikungunya transmitted by *Aedes aegypti* and *Aedes albopictus* showed that the transmission is likely to occur between 18-34°C with peak transmission between 26-29°C [43, 46, 47]. Moreover, the temperatures suitable for the transmission of the plant-borne disease, citrus greening, are between 16°C and 33°C with peak transmission at 25°C [48]. Together with our findings, this shows that there are similarities between ectotherm vectors in the way they respond to temperature. For example, their traits follow humped-shaped thermal performance curves. But there are differences in the temperature ranges they tolerate, and the temperatures at which their performance is maximal. This points to the importance of building system-specific models for predicting the effect of extrinsic factors on the spread of VBDs.

As highlighted in a 2018 systematic review [49], BTV has been studied using many different modeling approaches. The systematic review summarized BTV models used post-1998 [49], most of which relied more on strong modeling assumptions than data. The model results were used to inform animal health decision-making by identifying at-risk areas and the risk of spread in case of introduction [50], and climate change [45]. While several studies have examined R_0 for BTV [10, 22], our model differs in that it incorporates temperature

across a wide range, leading to estimating an R_0 that is also temperature-dependent. A more recent study used a mathematical quantity called vectorial capacity to estimate BTV transmission instead of R_0 [51]. R_0 and vectorial capacity are very similar, with the latter assuming perfect competence and ignoring host recovery rates (making our suitability metric somewhere in between). The study identifies the optimal transmission suitability range for *C. sonorensis* to be between 27 and 30 °C which overlaps with our transmission peak range of 26 and 29 °C. The difference is likely due to our study including trait data for two *Culicoides spp.* as well as including temperature-dependent infection parameters. Overall, both models are in agreement regarding the gross patterns of temperature effects BTV transmission.

In addition, while data on *Culicoides spp.* temperature dependent traits are scarce, we had the luxury of obtaining sufficient data to create a model for two North American vectors, and not mix traits across species from different continents. This is of particular interest in assessing the potential for invasion and establishment (and hence spread) of disease vectors, which has been found to be almost a hallmark of *Culicoides spp.* across the European landscape in recent decades, leading to novel outbreaks of BTV. Linking R_0 or $S(T)$ to temperature can help identify BTV outbreak risk based on the temperature at particular locations, which in turn can inform management policies and control strategies, within current and changing climate conditions. By establishing a model specific to current vectors in the U.S., we can assess the potential for invasion and spread to other parts of the globe.

Declarations

Ethics approval and consent to participate

Not applicable.

Consent for publication

Not applicable.

Availability of data and materials

All data generated or analyzed during this study are included in this published article and its supplementary information files.

Competing interests

The authors declare that they have no competing interests.

Funding

L.R.J. and F.E.M were partially supported by the National Science Foundation Career grant (NSF DMSDEB #1750113) and by National Institutes of Health, NIH-USDA, Ecology of Infectious Diseases (Award Number 1518681).

Authors' Contributions

F.E.M. and L.R.J. designed the study. F.E.M., H.S., and Z.T. collected the data from the literature and performed the Bayesian analyses. F.E.M and L.R.J. performed the mathematical analyses and S.J.R. performed the spatial mapping. F.E.M. wrote the paper. All authors contributed to revising and editing the paper and gave approval for publication.

Acknowledgements

Not applicable.

References

[1] E. A. Mordecai, K. P. Paaijmans, L. R. Johnson, C. Balzer, T. Ben-Horin, E. de Moor, A. McNally, S. Pawar, S. J. Ryan, T. C. Smith, and K. D. Lafferty, "Optimal tempera-

ture for malaria transmission is dramatically lower than previously predicted," *Ecology letters*, vol. 16, no. 1, pp. 22–30, 2013.

[2] L. R. Johnson, T. Ben-Horin, K. D. Lafferty, A. McNally, E. Mordecai, K. P. Paaijmans, S. Pawar, and S. J. Ryan, "Understanding uncertainty in temperature effects on vector-borne disease: a Bayesian approach," *Ecology*, vol. 96, no. 1, pp. 203–213, 2015.

[3] R. A. Taylor, E. A. Mordecai, C. A. Gilligan, J. R. Rohr, and L. R. Johnson, "Mathematical models are a powerful method to understand and control the spread of Huanglongbing," *PeerJ*, vol. 4, p. e2642, 2016.

[4] M. S. Shocket, S. J. Ryan, and E. A. Mordecai, "Temperature explains broad patterns of Ross River virus transmission," *Elife*, vol. 7, p. e37762, 2018.

[5] E. A. Mordecai, J. M. Caldwell, M. K. Grossman, C. A. Lippi, L. R. Johnson, M. Neira, J. R. Rohr, S. J. Ryan, V. Savage, M. S. Shocket, *et al.*, "Thermal biology of mosquito-borne disease," *Ecology Letters*, vol. 22, no. 10, pp. 1690–1708, 2019.

[6] W. J. Tabachnick, C. T. Smartt, and C. R. Connelly, "Bluetongue," *UF IFSAS Extension*, 2008.

[7] C. Calisher and P. Mertens, "Taxonomy of African horse sickness viruses," in *African Horse Sickness*, pp. 3–11, Springer, 1998.

[8] P. Mellor, J. Boorman, and M. Baylis, "Culicoides biting midges: their role as arbovirus vectors," *Annual review of entomology*, vol. 45, no. 1, pp. 307–340, 2000.

[9] E. Wittmann, P. Mellor, and M. Baylis, "Effect of temperature on the transmission of orbiviruses by the biting midge, Culicoides sonorensis," *Medical and veterinary entomology*, vol. 16, no. 2, pp. 147–156, 2002.

[10] S. Gubbins, S. Carpenter, M. Baylis, J. L. Wood, and P. S. Mellor, "Assessing the risk of bluetongue to UK livestock: uncertainty and sensitivity analyses of a temperature-

dependent model for the basic reproduction number," *Journal of the Royal Society Interface*, vol. 5, no. 20, pp. 363–371, 2007.

[11] K. A. Alexander, N. J. MacLachlan, P. W. Kat, C. House, S. J. O'Brien, N. W. Lerche, M. Sawyer, L. G. Frank, K. Holekamp, L. Smale, J. W. McNutt, M. K. Laurenson, M. G. L. Mills, and B. I. Osburn, "Evidence of natural bluetongue virus infection among african carnivores," *The American journal of tropical medicine and hygiene*, 1994.

[12] W. O. for Animal Health, "Bluetongue," *World Organisation for Animal Health (OIE)*, 2013.

[13] N. Preparedness, A. Incident Coordination Center, Veterinary Services, and P. H. I. Service, *Bluetongue standard operating procedure: an overview of etiology and ecology*, 2016.

[14] M. Jenckel, E. Bréard, C. Schulz, C. Sailleau, C. Viarouge, B. Hoffmann, D. Höper, M. Beer, and S. Zientara, "Complete Coding Genome Sequence of Putative Novel Bluetongue Virus Serotype 27," *Microbiology Resource Announcements*, vol. 3, no. 2, 2015.

[15] USDA, *Veterinary Biological Products*. United States Department of Agriculture, 2019.

[16] USDA, "U.S. Cattle & Beef Industry Statistics and Information," *Economic Research Service*, 2015.

[17] USDA, "Orbiviruses Gap Analysis: Bluetongue and Epizootic Hemorrhagic Disease," *Agricultural Research Service*, 2013.

[18] A. S. Lear and R. J. Callan, *Overview of Bluetongue*, 2014.

[19] N. J. MacLachlan and A. J. Guthrie, "Re-emergence of bluetongue, African horse sickness, and other Orbivirus diseases," *Veterinary Research*, 2010.

[20] EC, "Bluetongue seasonally vector free periods," *European Comission*, 2016.

[21] J. Turner, R. G. Bowers, and M. Baylis, "Two-host, two-vector basic reproduction ratio (R0) for bluetongue," *PloS one*, vol. 8, no. 1, p. e53128, 2013.

[22] S. P. Brand, K. S. Rock, and M. J. Keeling, "The interaction between vector life history and short vector life in vector-borne disease transmission and control," *PLoS computational biology*, vol. 12, no. 4, p. e1004837, 2016.

[23] R. Ross, *The prevention of malaria*. John Murray; London, 1911.

[24] G. Macdonald *et al.*, "The epidemiology and control of malaria.," *The Epidemiology and Control of Malaria.*, 1957.

[25] K. Dietz, "The estimation of the basic reproduction number for infectious diseases," *Statistical methods in medical research*, vol. 2, no. 1, pp. 23–41, 1993.

[26] O. Diekmann and J. A. P. Heesterbeek, *Mathematical epidemiology of infectious diseases: model building, analysis and interpretation*, vol. 5. John Wiley & Sons, 2000.

[27] O. Diekmann, J. A. P. Heesterbeek, and M. G. Roberts, "The construction of next-generation matrices for compartmental epidemic models," *Journal of the Royal Society Interface*, p. rsif20090386, 2009.

[28] A. I. Dell, S. Pawar, and V. M. Savage, "Systematic variation in the temperature dependence of physiological and ecological traits," *Proceedings of the National Academy of Sciences*, vol. 108, no. 26, pp. 10591–10596, 2011.

[29] M. J. Angilletta Jr and M. J. Angilletta, *Thermal adaptation: a theoretical and empirical synthesis*. Oxford University Press, 2009.

[30] W. J. Tabachnick, "*Culicoides variipennis* and bluetongue-virus epidemiology in the United States," *Annual Review of Entomology*, vol. 41, no. 1, pp. 23–43, 1996.

[31] J. A. Huwaldt and S. Steinhorst, "Plot digitizer," *URL http://plotdigitizer. sourceforge. net*, 2013.

[32] M. Plummer, *rjags: Bayesian Graphical Models using MCMC*, 2019. R package version 4-10.

[33] L. Joseph, D. B. Wolfson, and R. D. Berger, "Sample size calculations for binomial proportions via highest posterior density intervals," *Journal of the Royal Statistical Society: Series D (The Statistician)*, vol. 44, no. 2, pp. 143–154, 1995.

[34] R Development Core Team, *R: A Language and Environment for Statistical Computing*. R Foundation for Statistical Computing, Vienna, Austria, 2008. ISBN 3-900051-07-0.

[35] R. J. Hijmans, S. E. Cameron, J. L. Parra, P. G. Jones, and A. Jarvis, "Very high resolution interpolated climate surfaces for global land areas," *International Journal of Climatology: A Journal of the Royal Meteorological Society*, vol. 25, no. 15, pp. 1965–1978, 2005.

[36] M. Gilbert, G. Nicolas, G. Cinardi, T. P. Van Boeckel, S. Vanwambeke, W. G. R. Wint, and T. P. Robinson, "Global sheep distribution in 2010 (5 minutes of arc)," 2018. https://doi.org/10.7910/DVN/BLWPZN.

[37] M. Gilbert, G. Nicolas, G. Cinardi, T. P. Van Boeckel, S. O. Vanwambeke, G. W. Wint, and T. P. Robinson, "Global distribution data for cattle, buffaloes, horses, sheep, goats, pigs, chickens and ducks in 2010," *Scientific data*, vol. 5, p. 180227, 2018.

[38] R. J. Hijmans, *raster: Geographic Data Analysis and Modeling*, 2019.

[39] R. J. Hijmans and J. van Etten, *raster: Geographic analysis and modeling with raster data. R package version 2.0–12*, 2012.

[40] R. Bivand and N. Lewin-Koh, *maptools: Tools for Handling Spatial Objects*, 2020. R package version 1.0-2.

[41] R. Bivand, T. Keitt, and B. Rowlingson, *rgdal: Bindings for the 'Geospatial' Data Abstraction Library*, 2021. R package version 1.5-23.

[42] S. J. Ryan, A. McNally, L. R. Johnson, E. A. Mordecai, T. Ben-Horin, K. Paaijmans, and K. D. Lafferty, "Mapping physiological suitability limits for malaria in Africa under climate change," *Vector-Borne and Zoonotic Diseases*, vol. 15, no. 12, pp. 718–725, 2015.

[43] S. J. Ryan, C. J. Carlson, E. A. Mordecai, and L. R. Johnson, "Global expansion and redistribution of Aedes-borne virus transmission risk with climate change," *PLoS Neglected Tropical Diseases*, vol. 13, no. 3, p. e0007213, 2019.

[44] A. M. Samy and A. T. Peterson, "Climate change influences on the global potential distribution of bluetongue virus," *PloS One*, vol. 11, no. 3, p. e0150489, 2016.

[45] A. E. Jones, J. Turner, C. Caminade, A. E. Heath, M. Wardeh, G. Kluiters, P. J. Diggle, A. P. Morse, and M. Baylis, "Bluetongue risk under future climates," *Nature Climate Change*, vol. 9, no. 2, p. 153, 2019.

[46] E. A. Mordecai, J. M. Cohen, M. V. Evans, P. Gudapati, L. R. Johnson, C. A. Lippi, K. Miazgowicz, C. C. Murdock, J. R. Rohr, S. J. Ryan, *et al.*, "Detecting the impact of temperature on transmission of Zika, dengue, and chikungunya using mechanistic models," *PLoS neglected tropical diseases*, vol. 11, no. 4, p. e0005568, 2017.

[47] S. J. Ryan, C. J. Carlson, B. Tesla, M. H. Bonds, C. N. Ngonghala, E. A. Mordecai, L. R. Johnson, and C. C. Murdock, "Warming temperatures could expose more than 1.3 billion new people to Zika virus risk by 2050," *Global Change Biology*, 2020.

[48] R. A. Taylor, S. J. Ryan, C. A. Lippi, D. G. Hall, H. A. Narouei-Khandan, J. R. Rohr, and L. R. Johnson, "Predicting the fundamental thermal niche of crop pests and diseases in a changing world: a case study on citrus greening," *Journal of Applied Ecology*, vol. 56, no. 8, pp. 2057–2068, 2019.

[49] N. Courtejoie, G. Zanella, and B. Durand, "Bluetongue transmission and control in

Europe: A systematic review of compartmental mathematical models," *Preventive veterinary medicine*, 2018.

[50] N. Hartemink, B. Purse, R. Meiswinkel, H. E. Brown, A. De Koeijer, A. Elbers, G.-J. Boender, D. Rogers, and J. Heesterbeek, "Mapping the basic reproduction number (R0) for vector-borne diseases: a case study on bluetongue virus," *Epidemics*, vol. 1, no. 3, pp. 153–161, 2009.

[51] C. Mayo, E. McDermott, J. Kopanke, M. Stenglein, J. Lee, C. Mathiason, M. Carpenter, K. Reed, and T. A. Perkins, "Ecological dynamics impacting bluetongue virus transmission in north america," *Frontiers in Veterinary Science*, vol. 7, 2020.

[52] A. L. Lloyd, "Realistic distributions of infectious periods in epidemic models: changing patterns of persistence and dynamics," *Theoretical Population Biology*, vol. 60, no. 1, pp. 59–71, 2001.

[53] P. E. Parham and E. Michael, "Modeling the effects of weather and climate change on malaria transmission," *Environmental Health Perspectives*, vol. 118, no. 5, p. 620, 2010.

[54] T. J. Lysyk and T. Danyk, "Effect of temperature on life history parameters of adult Culicoides sonorensis (Diptera: Ceratopogonidae) in relation to geographic origin and vectorial capacity for bluetongue virus," *Journal of Medical Entomology*, vol. 44, no. 5, pp. 741–751, 2007.

[55] B. Mullens, A. Gerry, T. Lysyk, and E. Schmidtmann, "Environmental effects on vector competence and virogenesis of bluetongue virus in Culicoides: interpreting laboratory data in a field context," *Vet Ital*, vol. 40, no. 3, pp. 160–166, 2004.

[56] S. Carpenter, A. Wilson, J. Barber, E. Veronesi, P. Mellor, G. Venter, and S. Gubbins, "Temperature dependence of the extrinsic incubation period of orbiviruses in Culicoides biting midges," *PloS one*, vol. 6, no. 11, p. e27987, 2011.

[57] J. Vaughan and E. Turner Jr, "Development of immature Culicoides variipennis (Diptera: Ceratopogonidae) from Saltville, Virginia, at constant laboratory temperatures," *Journal of medical entomology*, vol. 24, no. 3, pp. 390–395, 1987.

[58] C. D. Harvell, C. E. Mitchell, J. R. Ward, S. Altizer, A. P. Dobson, R. S. Ostfeld, and M. D. Samuel, "Climate warming and disease risks for terrestrial and marine biota," *Science*, vol. 296, no. 5576, pp. 2158–2162, 2002.

A Appendix

A.1 Transmission model for BTV

We use an SIR-SEI type of compartmental model to describe vector-host interactions in transmitting BTV (see Figure 2). The host population (H) is divided into susceptible (S), infected (I), and recovered (or immune) (R) classes, while the vector population (V) is divided into susceptible (S_V) and infected (I_V) classes as well as three Exposed (E_V) classes. Here we use three exposed classes in the vector population to incorporate a more realistic length of the extrinsic incubation period. Using three compartments with the exit rate from each compartment being 3 ν, lead to a Gamma distribution for overall midge progression to the infectious class with a mean rate of ν. Increasing the number of compartments used from 3 to a larger number leads to a Gamma distribution with lower variance around the mean [52]. This approach is an alternative to using fixed time delays, which are not suitable when using temperature-dependent parameters. Both host (H) and vector (V) populations

are assumed (and are by definition of the model) constant.

$$\frac{dS}{dt} = -\frac{ab}{H} I_V S \tag{1}$$
$$\frac{dI}{dt} = \frac{ab}{H} I_V(t-\tau) S(t-\tau) - dI \tag{2}$$
$$\frac{dR}{dt} = dI \tag{3}$$
$$\frac{dS_V}{dt} = rV - \frac{ac}{H} I S_V - \mu S_V \tag{4}$$
$$\frac{dE_{V1}}{dt} = \frac{ac}{H} I S_V - 3\nu E_{V1} - \mu E_{V1} \tag{5}$$
$$\frac{dE_{V2}}{dt} = 3\nu E_{V1} - 3\nu E_{V2} - \mu E_{V2} \tag{6}$$
$$\frac{dE_{V3}}{dt} = 3\nu E_{V2} - 3\nu E_{V3} - \mu E_{V3} \tag{7}$$
$$\frac{dI_V}{dt} = 3\nu E_{V3} - \mu I_V. \tag{8}$$

where

$$H = S + I + R \tag{9}$$

$$V = S_V + E_{V1} + E_{V2} + E_{V3} + I_V \tag{10}$$

The model's parameters are presented in the Table 1 below. Note that the parameters

Parameter	Definition	Units
d	Recovery rate of infected hosts	1/day
τ	Host's exposure period	day
r	Vector population's birth rate	1/day
a	Vector biting rate	bites / day
b	Probability that a midge is infected	dimensionless
c	Probability that a midge is infectious	dimensionless
μ	Mortality rate of adult vectors	1/day
ν	Parasite's development rate	1/day

Table 1: Parameters used in the mathematical model, their description, and units.

609

610 τ is the time that a susceptible (S) takes to become infected after receiving a bite from
611 infected vector (I_V). The parameter ν is the inverse of the Extrinsic Incubation Period of

the pathogen (EIP), i.e., $\nu = \dfrac{1}{EIP}$. We define the vector population size to be $V = \dfrac{\lambda}{\mu}$, where λ is the total birth rate of adult midges in the whole population (adults/day), and μ is per-capita adult mortality rate (1/day). This is based on Parham & Michael [53], who derive the expression phenomenologically by treating V as a random variable. Thus, λ is equivalent to rV in the model above, given that $r = \mu$ at disease free equilibrium, and is given by

$$\lambda = \frac{F\ p_E\ p_L\ p_P}{(\rho_E + \rho_L + \rho_P)\ \mu} \tag{11}$$

where F is the number of eggs produced by all females in the population per day, $p_{E,L,P}$ are the survival probabilities in the Eggs, Larvae, and Pupae stages, and ρ_E, ρ_L, ρ_P are the development time in each stage. Then, the abundance of the vector becomes,

$$V = \frac{\lambda}{\mu} = \frac{F\ p_E\ p_L\ p_P}{(\rho_E + \rho_L + \rho_P)\ \mu^2} \tag{12}$$

A.2 Host recovery rate d sensitivity analysis

Although all ruminants are susceptible to BTV disease, each responds to the infection differently, with sheep being the most susceptible and showing extreme morbidity and mortality. In addition, BTV host recovery depends on the intensity of the infection as well as the time of disease detection, which results in recovery rate variability among hosts. To account for this, we perform a sensitivity analysis on the host recovery rate d by looking at the derivative of R_0 with respect to d as follows:

$$\frac{\partial R_0}{\partial d} = \frac{1}{2}\left(-\frac{V\ g\ f}{d^2\ H\ \mu}\right)\left(\frac{V\ g\ f}{d\ H\ \mu}\right)^{-1/2} = -\frac{1}{2d}\left(R_0^2\right)\left(R_0\right)^{-1} = -\frac{R_0}{2d}. \tag{13}$$

Since $\dfrac{\partial R_0}{\partial d} < 0$ always, the basic reproductive ratio R_0 increases as the recovery rate d decreases. Figure 1 shows different R_0 densities corresponding to different host recovery rate values. Higher lengths of infection $1/d$, i.e. lower recovery rates d, are associated with higher

631 R_0 densities, meaning that hosts with low recovery rate such as sheep are more challenging to manage as the chance of outbreak for them is more likely.

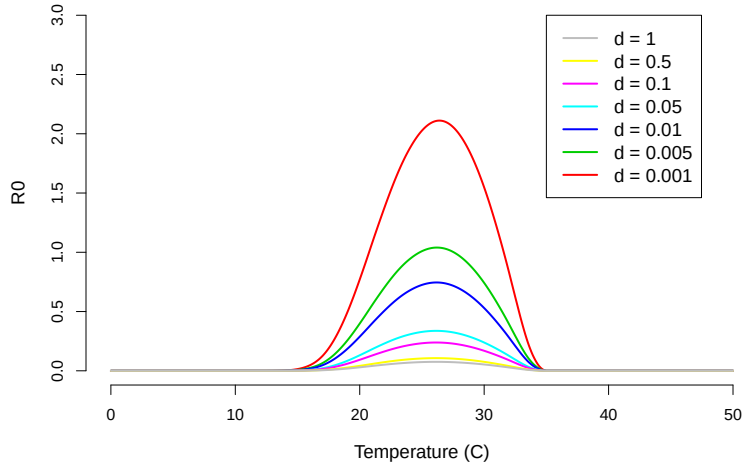

Figure 1: Host recovery rate d values correspond to different R_0 posterior densities. As d decreases, R_0 density increases meaning that a lower recovery rate correspond to a higher outbreak risk.

632

633 A.3 Uncertainty analysis

634 We investigate the uncertainty caused in each of R_0 components, the midge density V, the
635 functional form f, and the transmission potential g by examining the source of uncertainty
636 within each component. For the midge density, the uncertainty is mainly caused by the
637 adult midge mortality rate μ within a wide temperature range, from 10°C to 32°C. At
638 higher temperatures (¿32°C) the uncertainty is caused by the fecundity F.

639 In the functional form case, the uncertainty is caused by the adult mortality rate μ for
640 temperatures between 18°C and 32°C, this range overlaps with that of the midge density.
641 At lower (10-18°C) and higher (32-45°C) temperature ranges, the uncertainty is caused by
642 the pathogen development rate ν. In the transmission potential the overall uncertainty is
643 caused by the biting rate a.

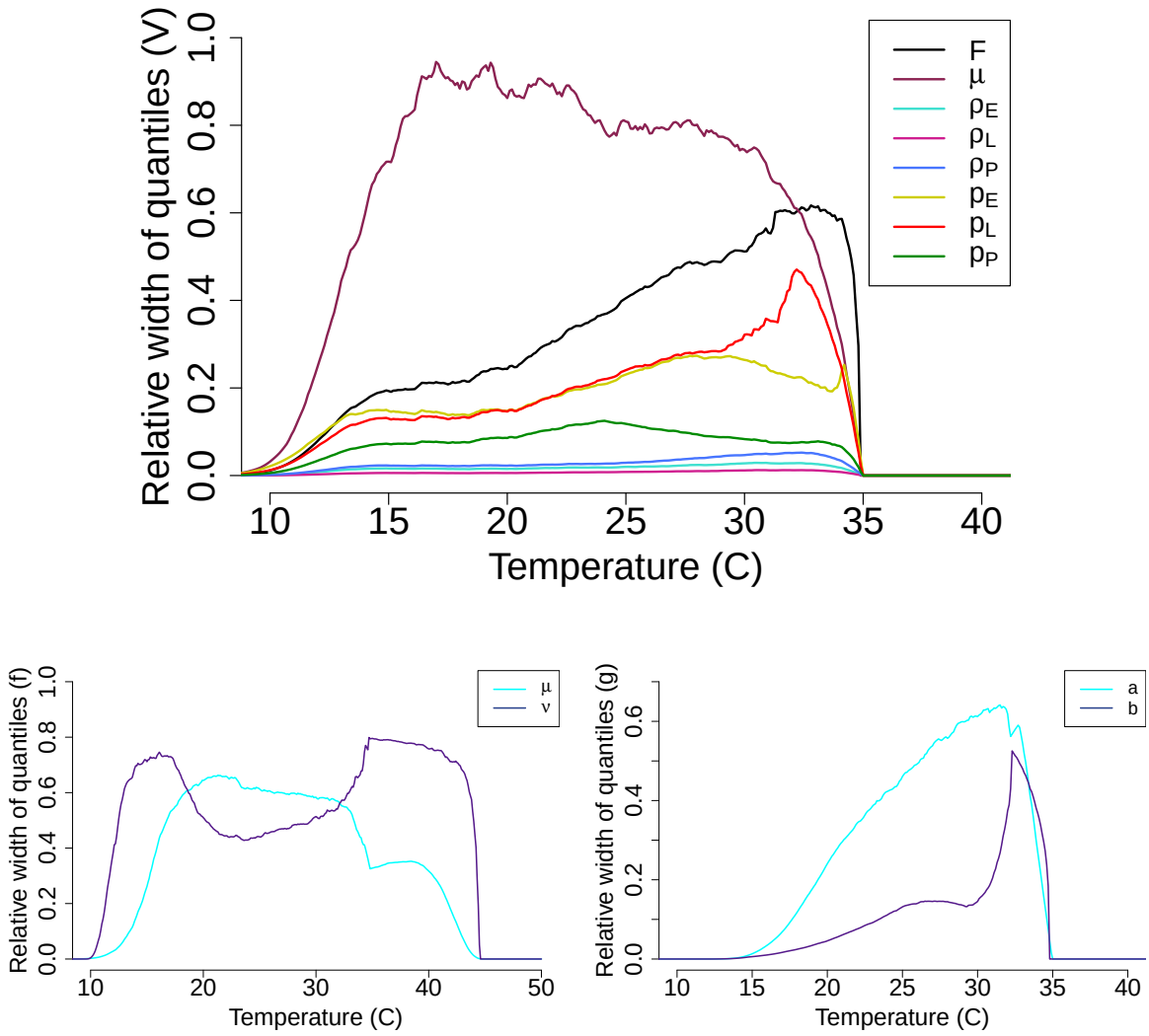

Figure 2: The source of uncertainty in the midge density V (Top), the functional form f (Bottom-left), and the transmission potential g (Bottom-right) is measured by calculating the relative width of quantiles with each parameter varying with temperature while the remaining parameters are kept constants.

A.4 Bayesian fitting of traits thermal curves

To fit each trait, we chose a unimodal functional form as the mean function. We use normal distributions for most of the data while binomial distributions are used when fitting probability distributions. We used uninformative priors appropriate for the biological description of the data, taking into account the positivity of their values as well as their range. The values in the priors are decided as we go until the appropriate fitting curve is obtained.

Midges biting rate a

The biting rate of adult midges is one of many factors that influence Bluetongue transmission [54]. In order to calculate the biting rate, the time required for female *Culicoides sonorensis* to lay eggs after a blood meal, also known as a gonotrophic period, is required. Biting rate (a) can be approximated by taking the inverse of the gonotrophic cycle duration. Similar to other traits, the biting rate is sensitive to environmental factors, especially, temperature [54] (see Figure 3 for thermal fit).

Vector competence bc

Vector competence for adult midges is a measure of their ability to transmit the disease. It is genetically determined and heavily influenced by environmental factors such as temperature and humidity [55]. Vector competence (bc) is the product of the probability of a vector getting infected after a blood meal containing a pathogen (c) and the probability of a vector transmiting infection (b). While we were able to find data for b concerning *Culicoides sonorensis* [56], we were unable to find data for c. We assume $c = 0.5$ for all calculations used in this analysis. We did fit a Bayesian model to the parameter b (Figure 4).

Juvenile survival probability $p_E,\ p_L,\ p_P$

Vaughan et. al. studied the sub-adult life cycle of *Culicoides variipennis* at temperatures of 20 °C, 25 °C, and 28 °C [57]. We define the probability of an egg hatching by using the mean percentage of laid eggs that hatched at each given temperature. We now define the probability of successful larval pupation by collecting the percentage of larva that ended up pupating at each given temperature. We finally define the probability of pupae emerging to become adults, p_P, as the mean percentage of pupae that survive to the adult stage at each given temperature (Figures 5, 6, 7).

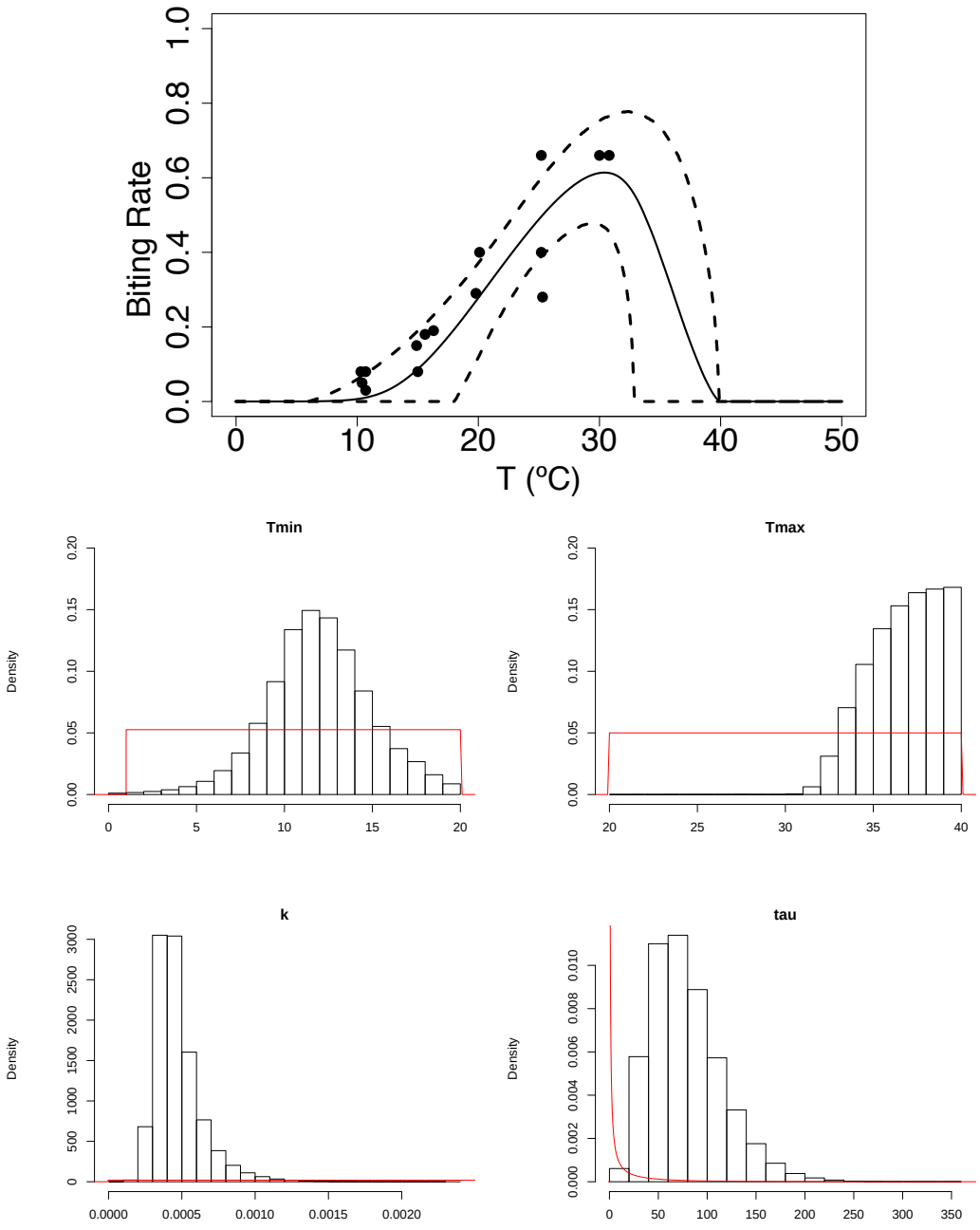

Figure 3: (Top) The mean trajectory in solid line and HPD interval in dashed black for the biting rate a. (Bottom) Histograms of the posterior distribution for each parameter of the Brière fit for the biting rate a. The prior distribution for each parameter is plotted in red. The Brière fit is determined by the equation $kT(T - T_{Min})\sqrt{T_{Max} - T}$ using a normal distribution with precision τ.

Juvenile development time $\rho_E,\ \rho_L,\ \rho_P$

Egg Development Time is defined as the time in days required for eggs to hatch in a given temperature. *Culicoides variiennis* were studied in a laboratory setting [57]. Larva Devel-

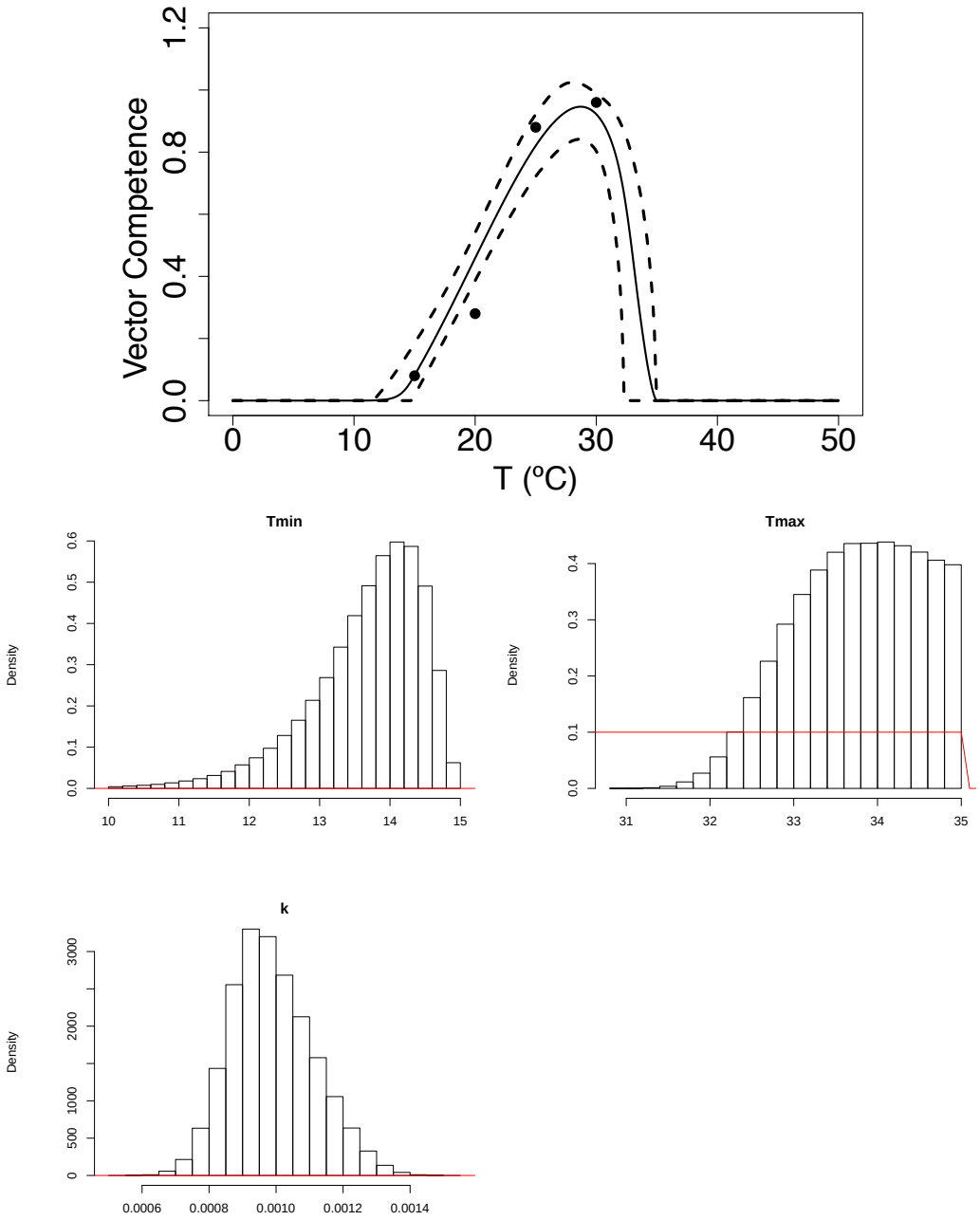

Figure 4: (Top) The mean trajectory in solid line and HPD interval in dashed black for the probability of a vector transmitting the virus when biting b. (Bottom) Histograms of the posterior distribution for each parameter of the Brière fit for the probability b. The prior distribution for each parameter is plotted in red. The Brière fit is determined by the equation $kT(T - T_{Min})\sqrt{T_{Max} - T}$ using a binomial distribution.

opment Time is defined as the time in days required for the larva to mature into a pupa in a given temperature. Pupa Development Time is defined as the time in days required for a

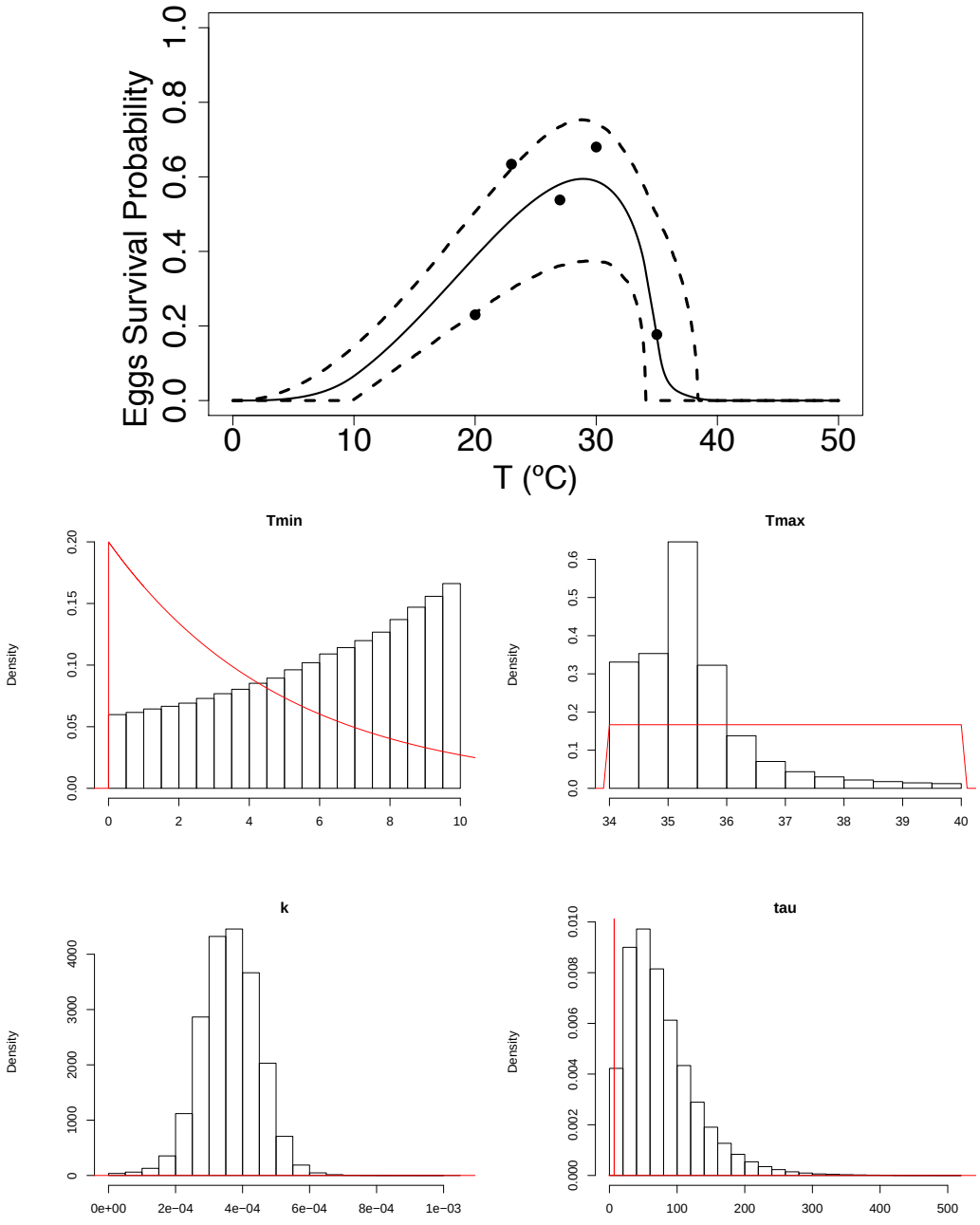

Figure 5: (Top) The mean trajectory in solid line and HPD interval in dashed black for the egg survival probability p_E. (Bottom) Histograms of the posterior distribution for each parameter of the Brière fit for the probability p_E. The prior distribution for each parameter is plotted in red. The Brière fit is determined by the equation $kT(T - T_{Min})\sqrt{T_{Max} - T}$ using a normal distribution with precision τ.

pupa to mature into adult midges in a given temperature (Figures 8, 9, 10).

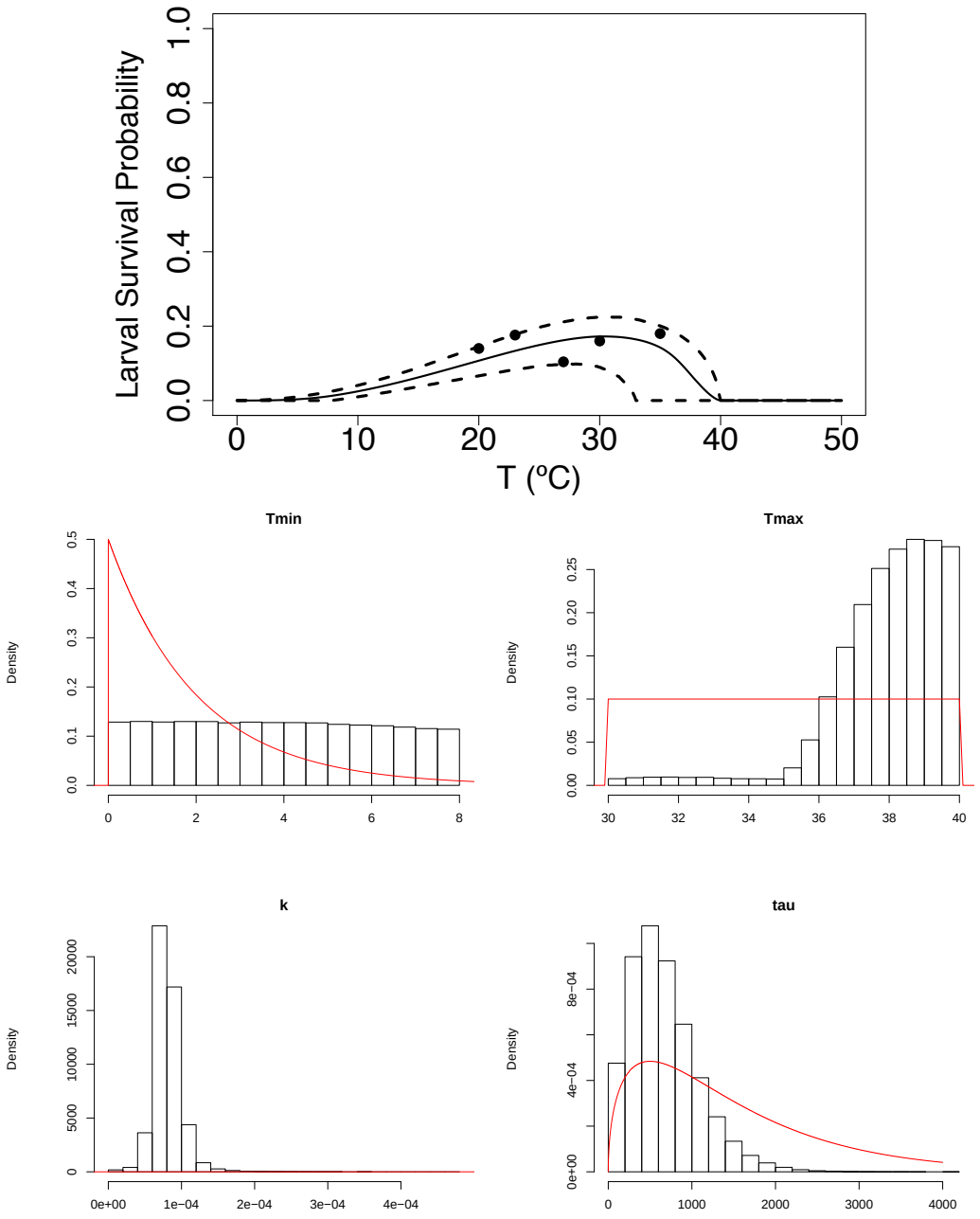

Figure 6: (Top) The mean trajectory in solid line and HPD interval in dashed black for the larval survival probability p_L. (Bottom) Histograms of the posterior distribution for each parameter of the Brière fit for the probability p_L. The prior distribution for each parameter is plotted in red. The Brière fit is determined by the equation $kT(T - T_{Min})\sqrt{T_{Max} - T}$ using a normal distribution with precision τ.

Fecundity F

The rate at which female midges lay eggs is closely related to the spread of Bluetongue. This rate is typically measured as eggs per female per day. For this study we also utilized fecundity

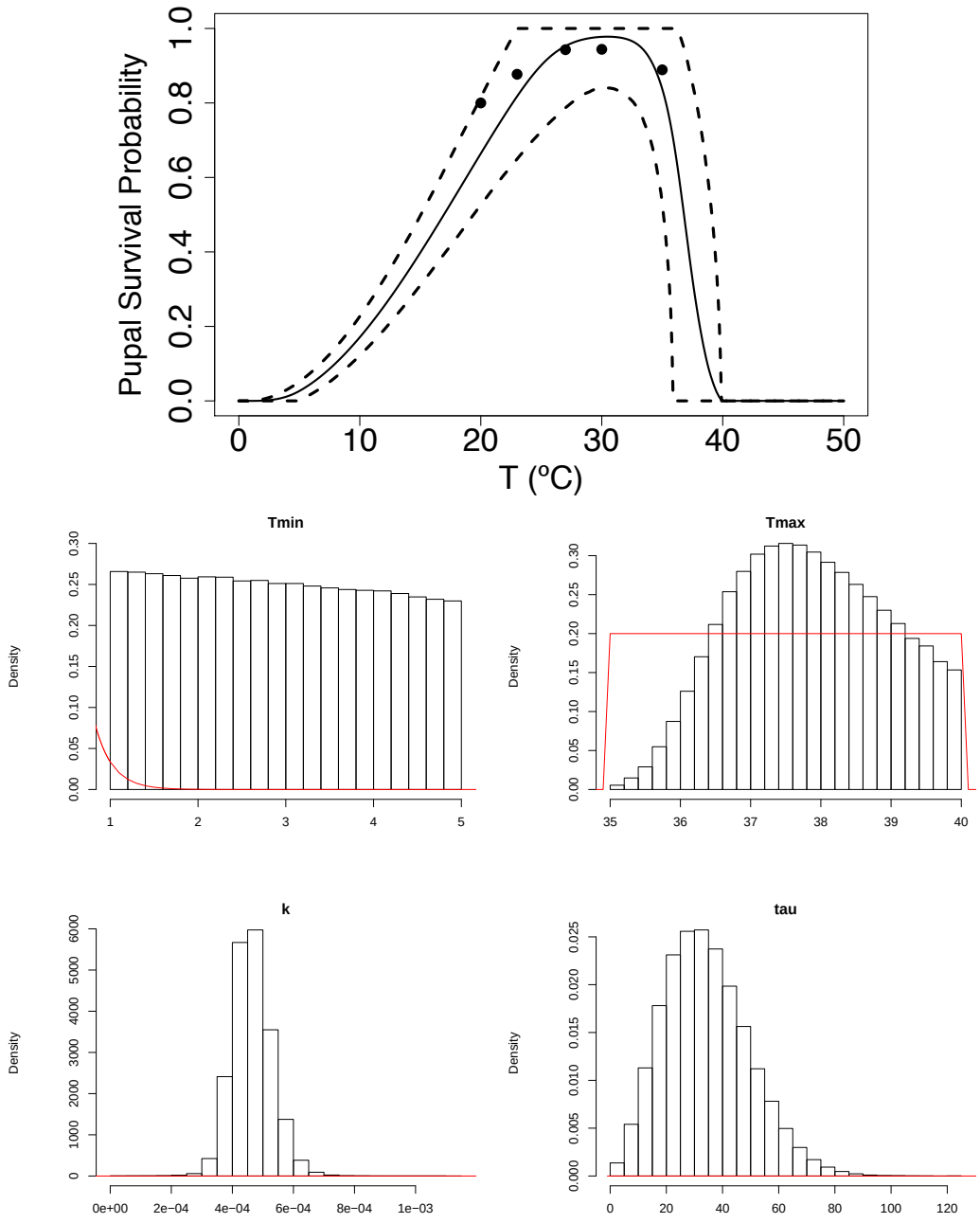

Figure 7: (Top) The mean trajectory in solid line and HPD interval in dashed black for the pupal survival probability p_P. (Bottom) Histograms of the posterior distribution for each parameter of the Brière fit for the probability p_P. The prior distribution for each parameter is plotted in red. The Brière fit is determined by the equation $kT(T - T_{Min})\sqrt{T_{Max} - T}$ using a normal distribution with precision τ.

682 data that was taken over two oviposition cycles and transformed the data (originally eggs
683 per female) by dividing by the median oviposition time [54].

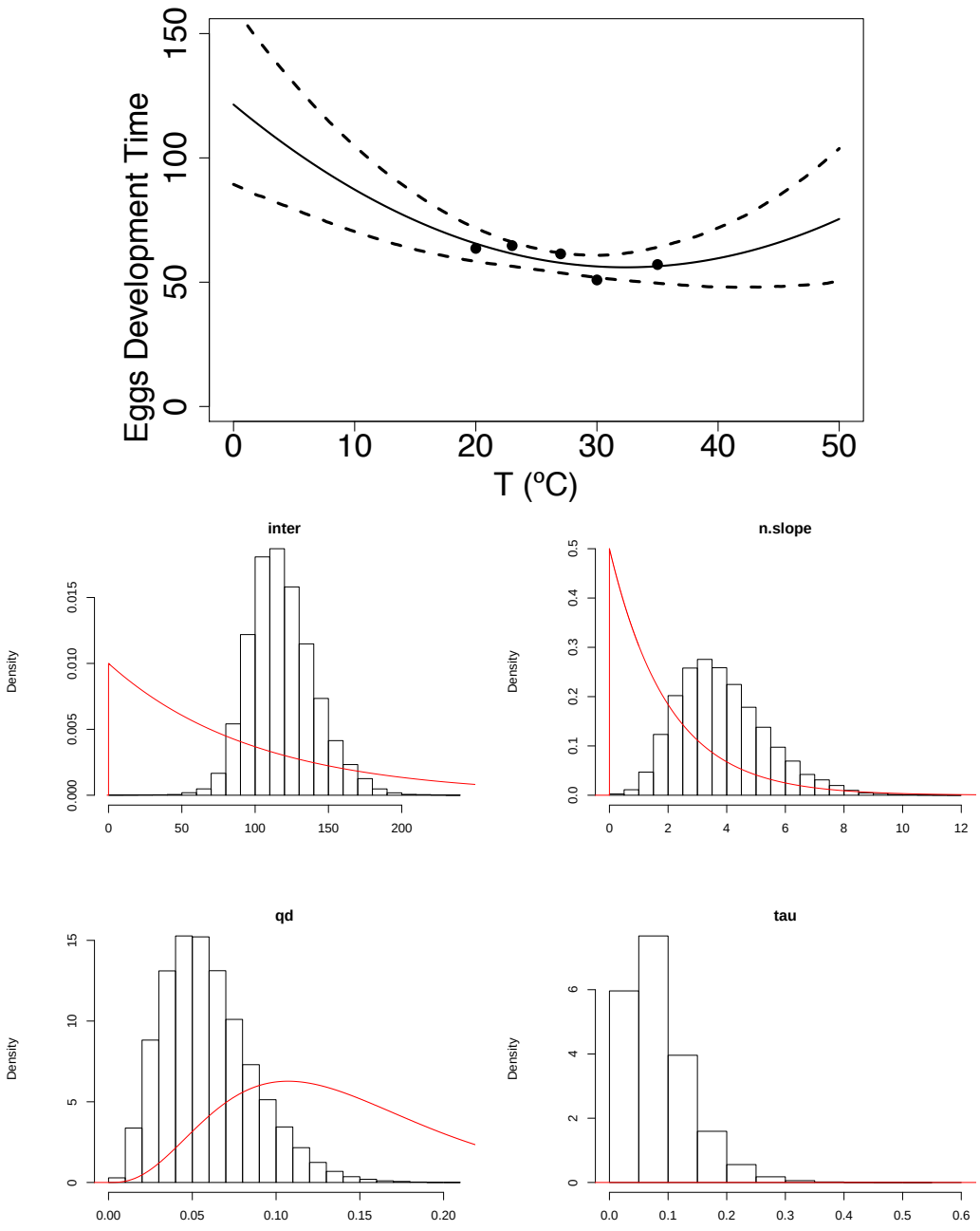

Figure 8: (Top) The mean trajectory in solid line and HPD interval in dashed black for egg development time ρ_E. (Bottom) Histograms of the posterior distribution for each parameter of the quadratic fit for egg development time ρ_E. The prior distribution for each parameter is plotted in red. The quadratic fit is determined by the equation $inter - n.slope\, T + qd\, T^2$ using a normal distribution with precision τ.

Pathogen development rate ν

Parasite development has been shown to increase with temperature in studies that support the hypothesis that global warming has been cause for latitudinal shifts which in turn increase

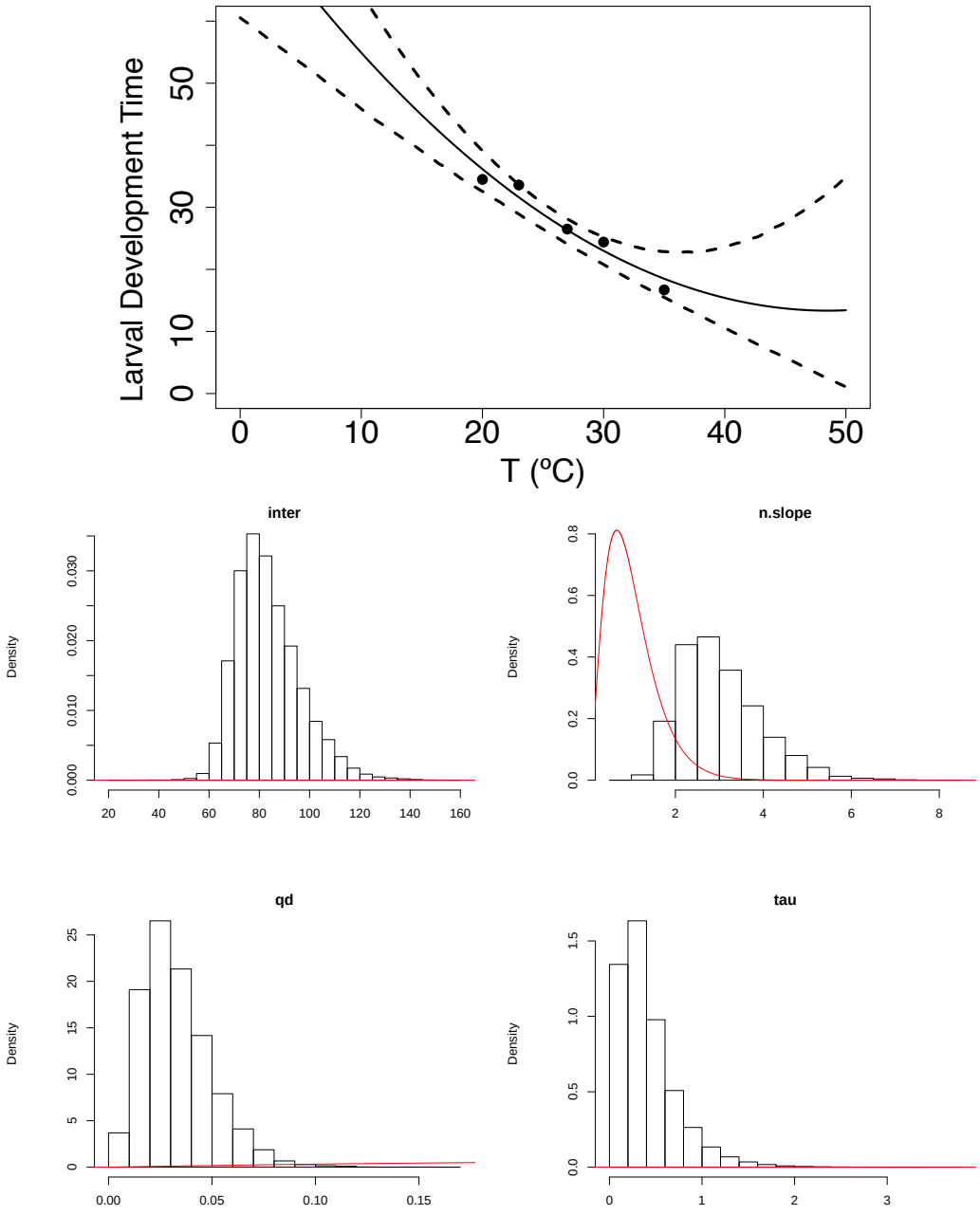

Figure 9: (Top) The mean trajectory in solid line and HPD interval in dashed black for larval development time ρ_L. (Bottom) Histograms of the posterior distribution for each parameter of the quadratic fit for larval development time ρ_L. The prior distribution for each parameter is plotted in red. The quadratic fit is determined by the equation $inter - n.slope\, T + qd\, T^2$ using a normal distribution with precision τ.

687 the reach of vectors that transmit diseases like bluetongue [58]. In order to investigate this
688 trait's relationship with temperature, we made use of data on Extrinsic Incubation Period
689 (EIP) to create a new parameter: Parasite Development Rate (ν) ($\nu = 1/\text{EIP}$). EIP is the

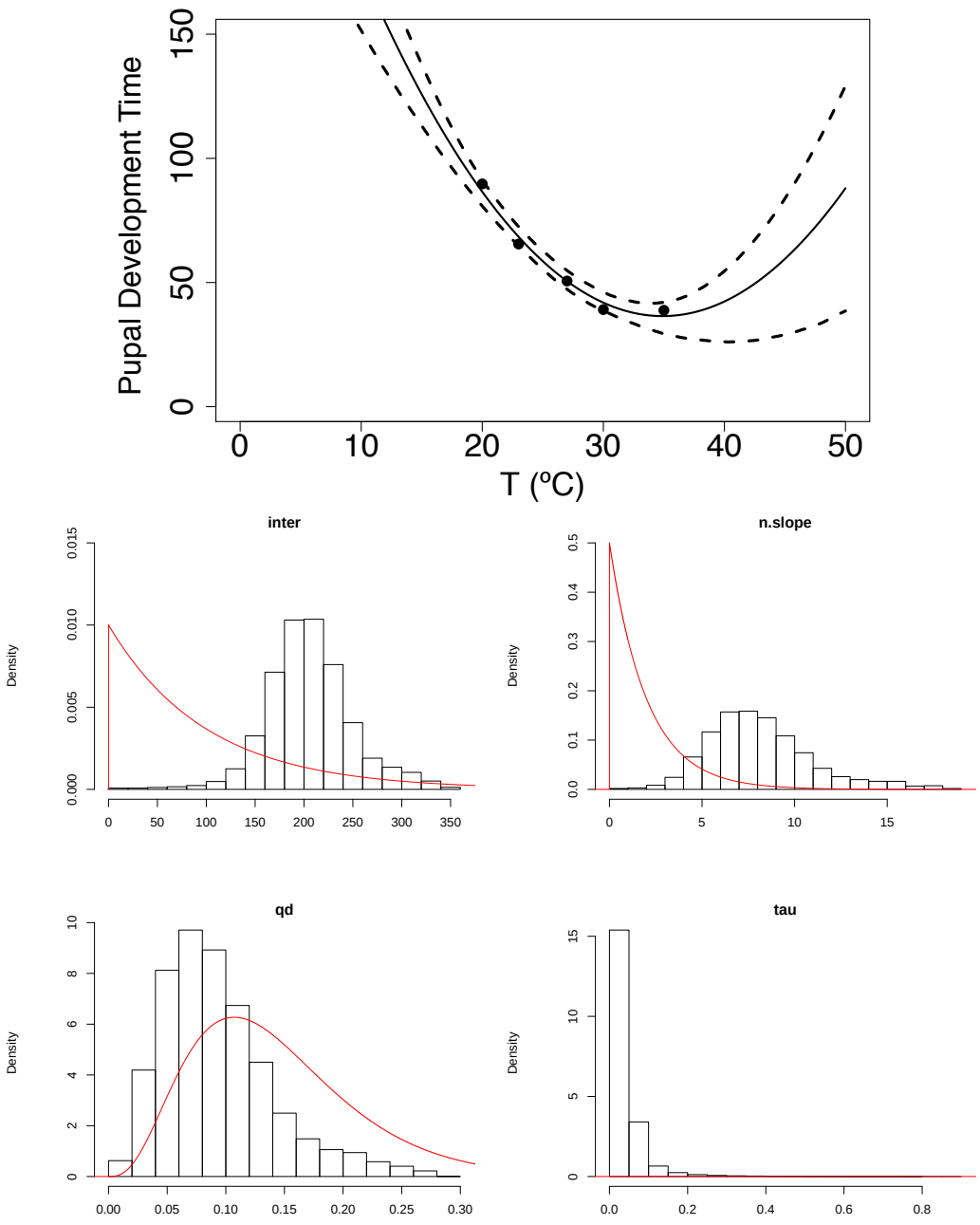

Figure 10: (Top) The mean trajectory in solid line and HPD interval in dashed black for pupal development time ρ_P. (Bottom) Histograms of the posterior distribution for each parameter of the quadratic fit for pupal development time ρ_P. The prior distribution for each parameter is plotted in red. The quadratic fit is determined by the equation $inter - n.slope\, T + qd\, T^2$ using a normal distribution with precision τ.

time between a vector getting infected with a pathogen to the time that the vector itself is able to transmit the pathogen.

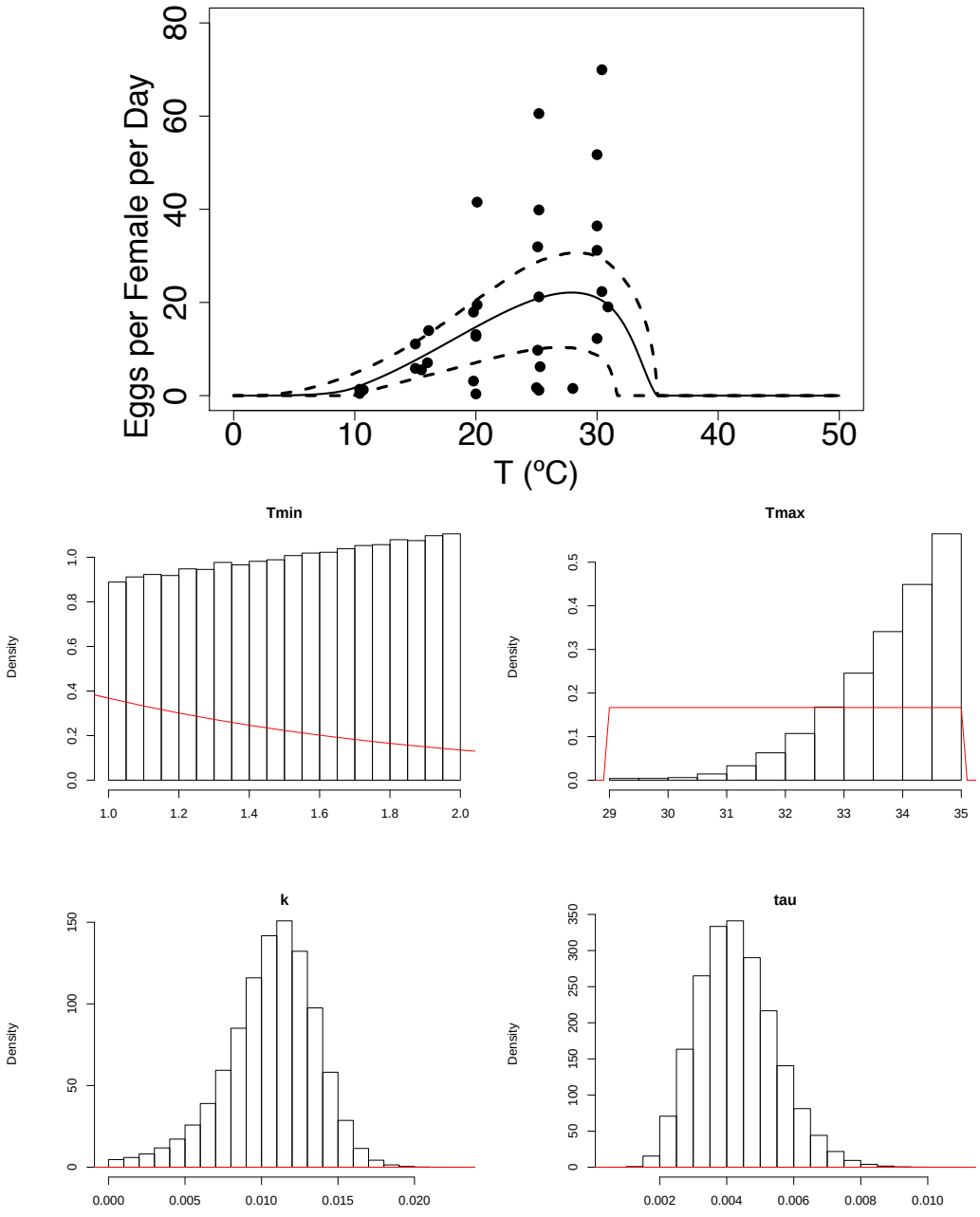

Figure 11: (Top) The mean trajectory in solid line and HPD interval in dashed black for fecundity F. (Bottom) Histograms of the posterior distribution for each parameter of the Brière fit for fecundity F. The prior distribution for each parameter is plotted in red. The Brière fit is determined by the equation $kT(T - T_{Min})\sqrt{T_{Max} - T}$ using a normal distribution with precision τ.

Adult mortality rate μ

The rate at which midges die over a span of time is known as the mortality rate μ. We define the mortality rate of midges as $\frac{1}{lf}$, where lf represents the lifespan of midges in days,

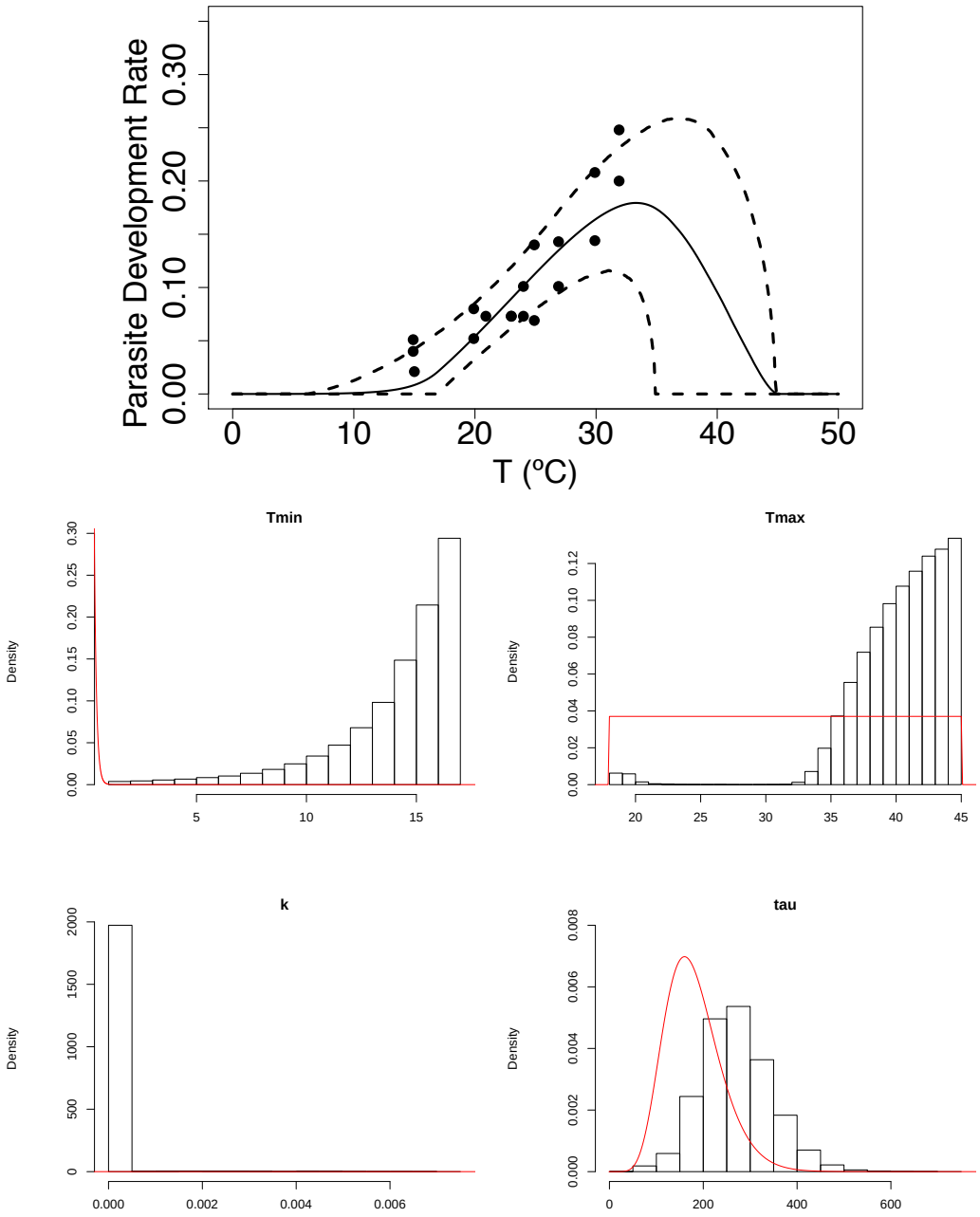

Figure 12: (Top) The mean trajectory in solid line and HPD interval in dashed black for the parasite development rate ν. (Bottom) Histograms of the posterior distribution for each parameter of the Brière fit for the parasite development rate ν. The prior distribution for each parameter is plotted in red. The Brière fit is determined by the equation $kT(T - T_{Min})\sqrt{T_{Max} - T}$ using a normal distribution with precision τ.

or the probability of survival for the midges. We define mortality rate in the case where lf is the lifespan of midges in days. Mortality rate is also sensitive to environmental factors, especially temperature [54].

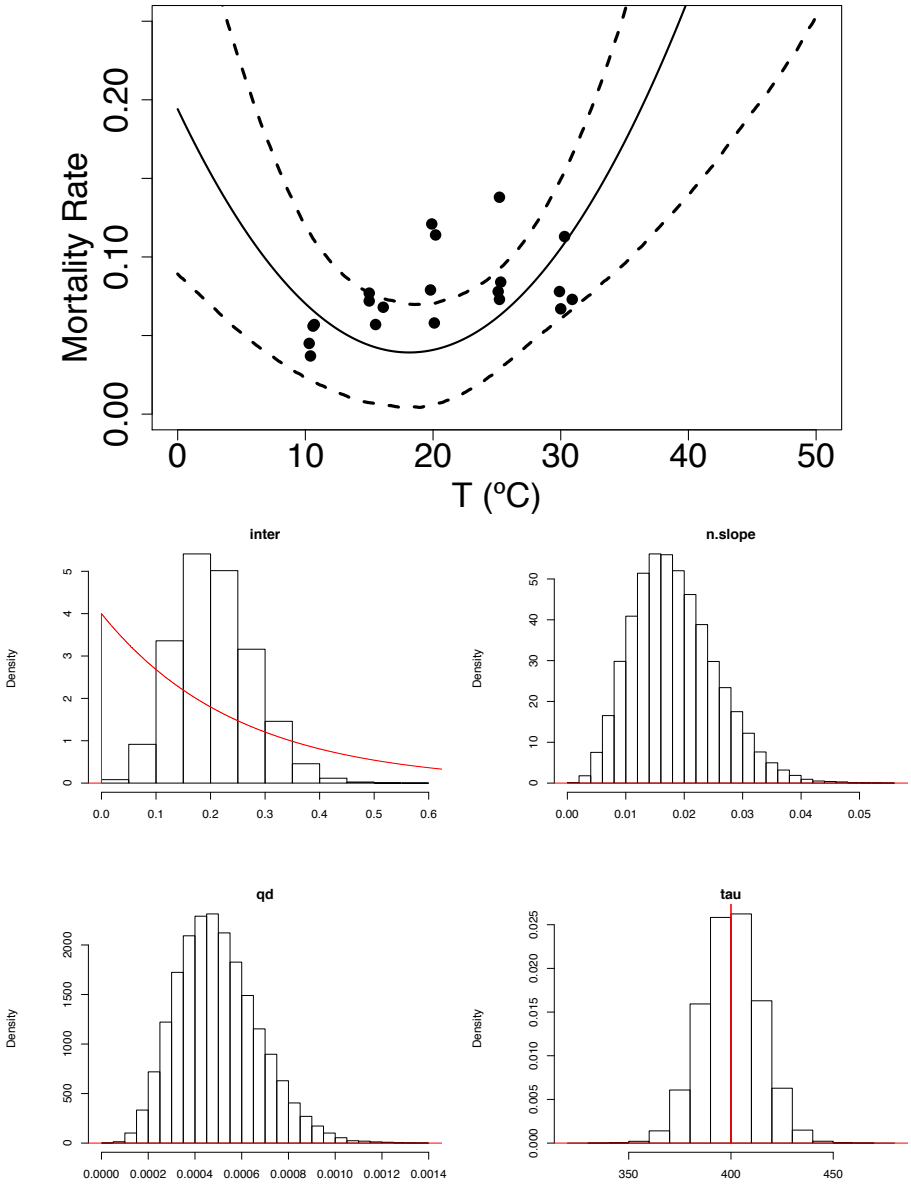

Figure 13: (Top) The mean trajectory in solid line and HPD interval in dashed black for the mortality rate μ. (Bottom) Histograms of the posterior distribution for each parameter of the quadratic fit for the mortality rate μ. The prior distribution for each parameter is plotted in red. The quadratic fit is determined by the equation $inter - n.slope\, T + qd\, T^2$ using a normal distribution with precision τ.

Thermal traits prior distributions

Table 2 summarizes all the priors used to fit the thermal curves.

A.5 Posterior distributions for all $S(T)$ forms

For all three R_0 posterior distributions we provide posterior distributions for the lower temperature limit, peak temperature, and upper temperature limit.

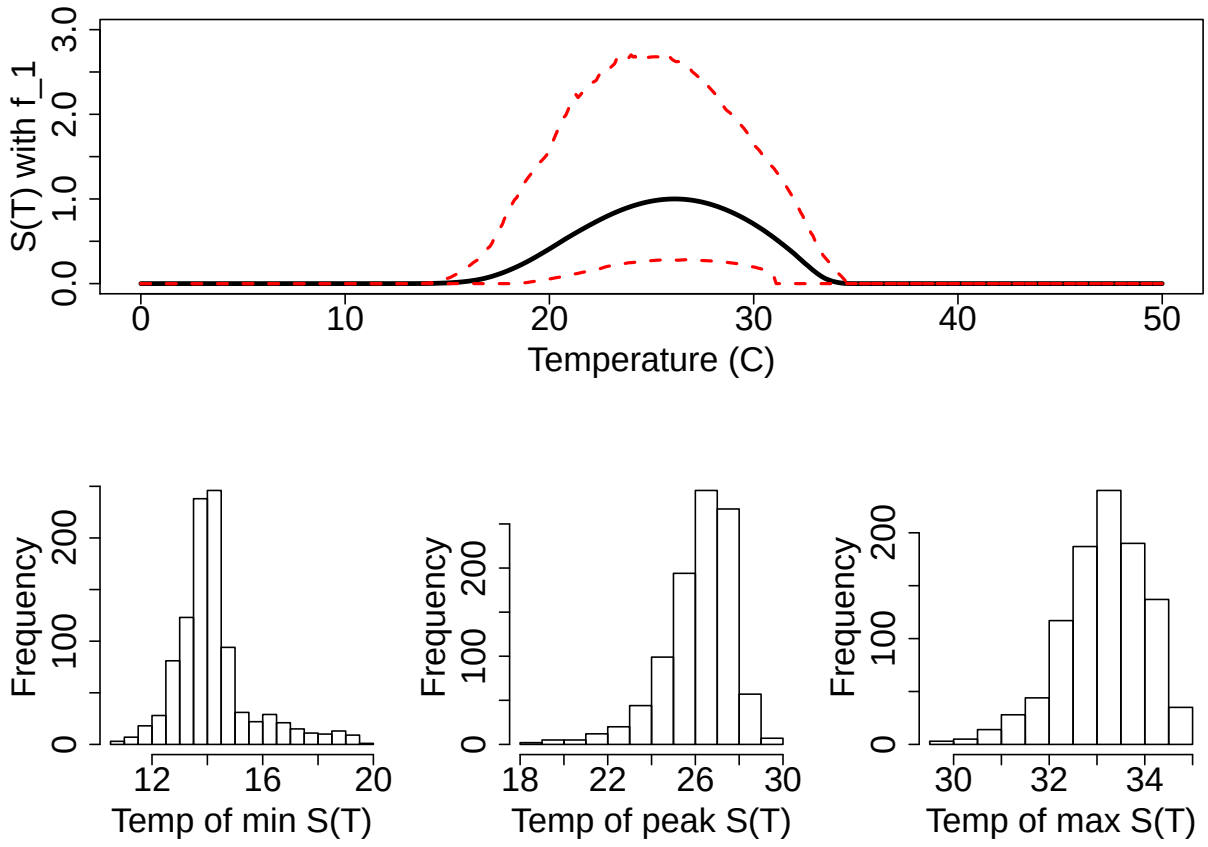

Figure 14: Minimum, peak and, maximum temperatures posterior densities for Dietz 1993 [25] R_0

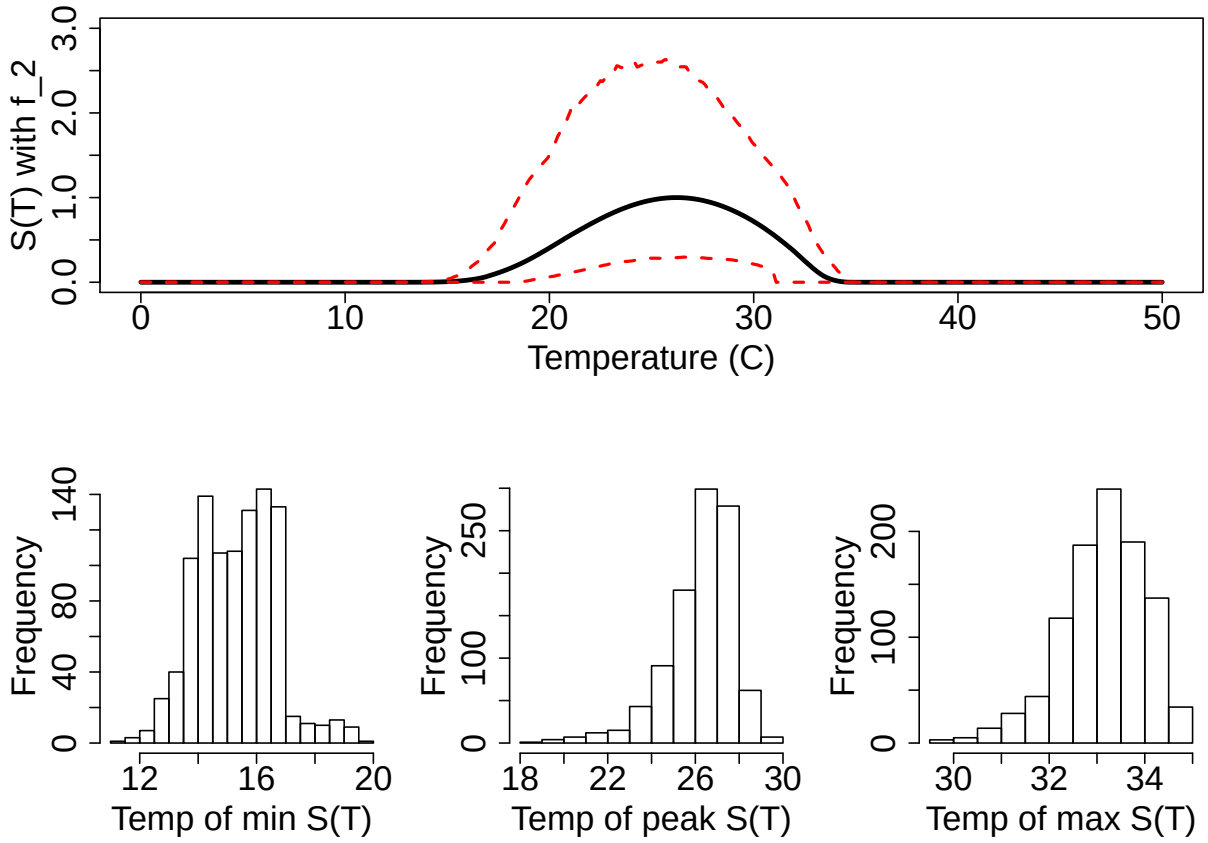

Figure 15: Minimum, peak and, maximum temperatures posterior densities for Gubbins 2008 [10] R_0

A.6 Digitized data

Table 3 shows the digitized trait values and their corresponding references.

Parameter	Trait	Value	Units	Transformed	Ref.
a	Vector biting rate	0.05	bites/day	Y	48
		0.03			
		0.08			
		0.18			
		0.29			
		0.4			
		0.4			

		0.28 0.28 0.66 0.66 0.08 0.08 0.15 0.19 0.66			
b	Probability of transmission	0.08 0.28 0.28 0.88 0.96	dimensionless	Y	50
efd	Fecundity	5.528 3.122 13.11 9.745 6.206 31.191 19.034 1.361 1.242 11.08 13.961 17.93 41.531	# eggs per female per day	Y	48

		60.535			
		39.856			
		51.724			
		69.951			
		12.731			
		1.154			
		36.417			
		0.465			
		5.844			
		7.048			
		19.469			
		31.938			
		21.195			
		12.255			
		22.332			
		0.365			
		1.703			
		1.536			
edt	Egg's development time	63.6	Days	N	51
		64.7			
		61.4			
		50.9			
		57.1			
ldt	Larva's development time	34.5	Days	N	51
		33.6			
		26.5			
		24.4			

		16.7			
$PuDt$	Pupa's development time	89.7 65.5 50.6 39.1 38.8	Days	N	51
μ	Adult's mortality rate	0.037 0.057 0.072 0.057 0.121 0.058 0.078 0.084 0.067 0.073 0.045 0.056 0.077 0.068 0.079 0.114 0.138 0.073 0.078 0.113	$\frac{1}{\text{Days}}$	Y	48
pdr	Extrinsic incubation	0.051	$\frac{1}{\text{Days}}$	Y	52

	period (EIP)	0.04 0.021 0.052 0.08 0.073 0.073 0.073 0.073 0.069 0.101 0.101 0.14 0.143 0.144 0.208 0.2 0.248			
pE	Egg's survival probability	0.23 0.634 0.538 0.68 0.177	dimensionless	N	51
pL	Larva's survival probability	0.14 0.176 0.104 0.16 0.18	dimensionless	N	51

pP	Pupa's survival Probability	0.8 0.877 0.943 0.944 0.889	dimensionless	N	51

Table 3: Traait values digitized and fit using MCMC.

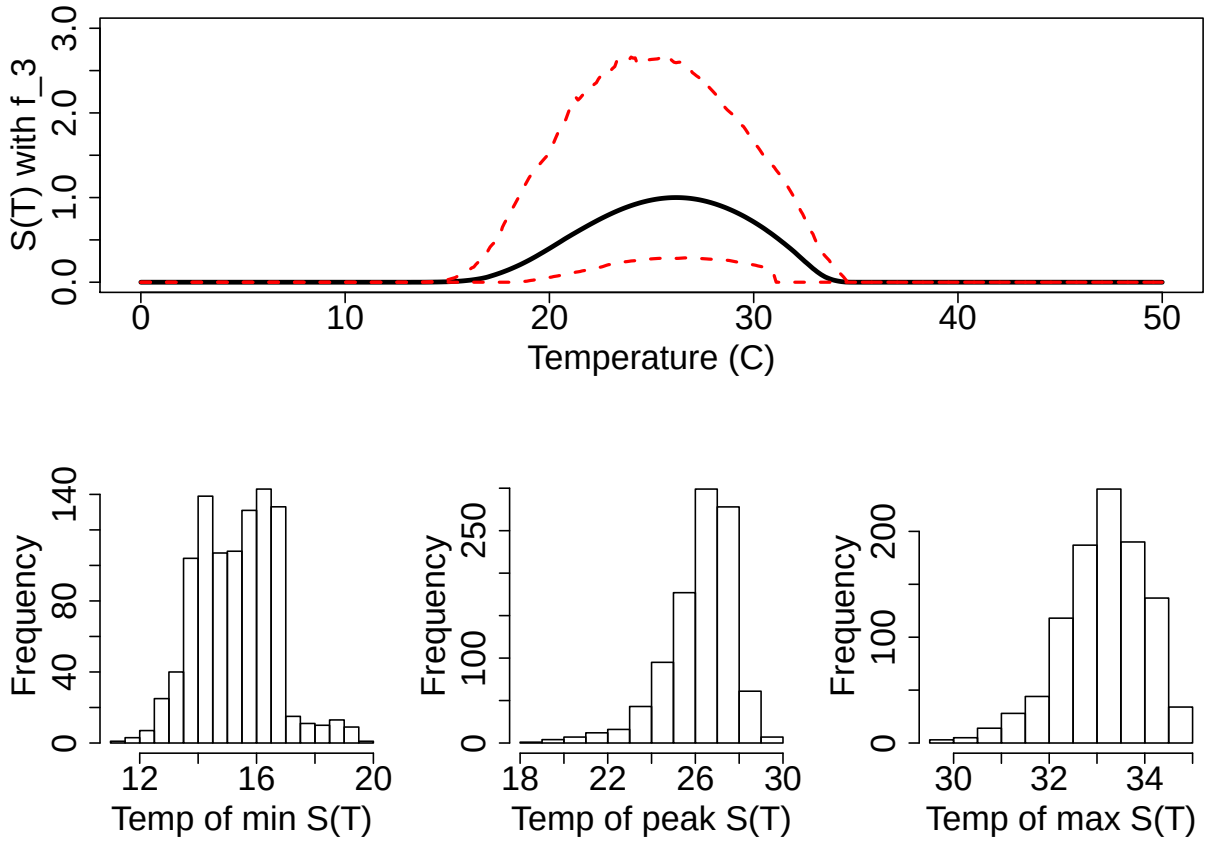

Figure 16: Minimum, peak and, maximum temperatures posterior densities for the R_0 presented here.

Model Parameter	Mean Function	Parameters	Prior
Biting Rate		T_{Min}	dunif(0, 20)
a	Brière	T_{Max}	dunif(20,40)
		k	dgamma(1,20)
		τ	dgamma(0.01, 0.01)
Transmission probability		T_{Min}	dunif(10,24)
b	Brière	T_{Max}	dunif(25,35)
		k	dgamma(1,10)
Egg Survival Probability		T_{Min}	dunif(10,20)
p_E	Brière	T_{Max}	dunif(35,40)
		k	dgamma(1,20)
		τ	dgamma(7, 5^{-10})
Larval Survival Probability		T_{Min}	dunif(0,8)
p_L	Brière	T_{Max}	dunif(30,40)
		k	dgamma(1,20)
		τ	dgamma(1.5, 0.001)
Pupal Survival Probability		T_{Min}	dunif(1,5)
p_P	Brière	T_{Max}	dunif(35,40)
		k	dgamma(1,5)
		τ	dgamma(10, 0.002)
Egg Development Time		inter	dgamma(1, 0.01)
ρ_E	Quadratic	n.slope	dgamma(1, 0.5)
		qd	dgamma(4,28)
		τ	dnorm(3, 1/800)
Larval Development Time		inter	dgamma(1, 0.01)
ρ_L	Quadratic	n.slope	dgamma(1, 0.5)
		qd	dgamma(4,28)
		τ	dnorm(3, 1/1000)
Pupal Development Time		inter	dgamma(1, 0.01)
ρ_P	Quadratic	n.slope	dgamma(1, 0.5)
		qd	dgamma(4,28)
		τ	dnorm(3, 1/200)
Eggs per Female per Day		T_{Min}	dunif(1, 10)
F	Brière	T_{Max}	dunif(29,35)
		k	dgamma(1,1)
		τ	dgamma(9, 0.0005)
Parasite Development Rate		T_{Min}	dunif(1, 17)
ν	Brière	T_{Max}	dunif(18,45)
		k	dgamma(1,10)
		τ	dgamma(9, 0.05)
Adult Mortality Rate		inter	dgamma(2,2)
μ	Quadratic	n.slope	dgamma(3,3)
		qd	dgamma(2,2)
		τ	dnorm(1000, 1/500)

Table 2: Prior distributions for each of the parameters for the fitting of the responses for each of the thermal traits considered.